




University of
Stavanger

Faculty of Science and Technology

MASTER THESIS

Study program/Specialization: Master of Science in Engineering Structure and Materials Engineering / Mechanical System	Spring semester, 2021 Open access
Authors: Ankit Awadesh Pandey	 (Author's signature)
Faculty supervisor: Mudiyan Nirosha Damayanthi	
External supervisor(s):	
Thesis Title: Effect of Hydrogen on the Mechanical Properties of High Strength Steel.	
Credits (ECTS): 30	
Key words: Embrittlement Charging Cathodic Protection Hydrogen Induced Cracking Tensile Testing Slow strain Rate method	Pages:35..... + enclosure: 9 Stavanger,14/07/2021..... Date/year

Preface

Our aspirations in choosing to work with hydrogen effect on the mechanical properties of high strength carbon steel was to deliver solid data for analysis and a thesis useful for all the applications. The best way to start this work was by structured planning and good teamwork. Therefore, our first task on the agenda was creation of a detailed project timeline, including late and early finish for all tasks. This gave us a good overview throughout the project and kept our demand for quality peaking from start to finish. The next task on the agenda was to set the number of test samples to the maximum, maximizing our data, which is the overall goal. If our conclusions of the thesis should be considered valid, we needed enough data.

Both these decisions helped lift the work with the thesis up to the acquired level of quality we wanted.

Abstract

The main purpose of this experiment is to compare the mechanical properties of hydrogen charged and uncharged samples. This thesis work started with the machining samples of AISI 1074 rectangular bar into tensile test specimen. This whole process involved cutting, machining, heat treatment, tempering and this results to 17 samples for tensile test. To obtain this all the specimens were heated at 900 degree Celsius for 30 minutes and quenched into the oil. Later on different samples were tempered at different temperature as per the selection. They were split into 3 groups, where 2 groups were hydrogen charged with different time durations. Vickers hardness test is used to measure hardness of different samples.

The next step is to induced hydrogen inside the samples for certain period of time by placing into the electrolyte with distilled water 3.5 wt. % NaCl. The sample had each an incubation period of between 14-20 days assuming sufficient hydrogen diffusion after 2 weeks. The samples from group 2 and group 3 were hydrogen charged which is done by designing and machining a canister to surround the specimen during testing where group 1 were tested in air with normal strain rate. This samples underwent normal tensile test to determine the elastic modulus, yield strength of the material. And the other group of rods were immersed inside the 3.5 wt. % NaCl and subjected to the cathodic protection, where titanium electrode were used as counter electrode for the diffusion of hydrogen inside the sample. Results were compared between all series shows clear indication of hydrogen embrittlement in group 2 and group 3

Contents

Preface.....	1
Abstract.....	2
Acknowledgements	1
Abbreviations	2
Introduction.....	3
1. Theoretical Background.....	6
1.1 Overview of the Chapter	6
1.2 Diffusion of hydrogen	6
1.2.1 Hydrogen Enhanced Decohesion Mechanism	7
1.2.2 Hydrogen Enhanced local plasticity	8
1.2.3 Hydrogen Enhanced Macroscopic Ductility (HEMP)	8
1.3 Effect of hydrogen on the mechanical properties of steel	9
1.4 Ductility.....	9
1.5 Heat Treatment	9
1.6 Tempering.....	11
1.7 Vickers Hardness test	12
1.8 Tensile Testing.....	12
1.9 Cathodic Protection	13
2. Experimental Work	14
2.1 Chemical Composition and Cutting Process	14
2.2 CNC of Samples	15
2.3 Setting Serials number on Samples	16
2.4 Heat treatment and quenching	17
2.5 Hardness test after hardening the samples.....	18
2.6 Tempering.....	18
2.7 Sample preparation for hardness test	19
2.8 Electrolysis.....	19
2.9 Tensile test under cathodic protection	21
3. Results	23
3.1 Vickers Hardness Testing.....	23
3.2 Tensile test under cathodic protection	26
3.2.1 Tensile Test in Air (Series 1)	26
3.2.2 Tensile test for hydrogen charged Sample (Series 2 and Series 3).....	28

3.3 Comparison of different factors	29
3.4 Susceptibility of hydrogen embrittlement	32
4. Discussion.....	35
4.1 Errors in designing and machining of samples	35
4.2 Heat treatment and tempering levels	35
4.3 Hydrogen Charging	36
4.4 Slow strain rate test	36
4.5 Tensile test results	36
5. Conclusion	37
References.....	38

Acknowledgements

First of all, I wish to thank my thesis supervisor Mudiyan Nirosha Adasooriya, by the University of Stavanger, for an interesting and challenging thesis. His expertise on hydrogen embrittlement and related areas have been a great help and inspiration in writing this thesis.

Secondly, I also want to thank Johan Andreas Thorikaas for great guidance and help in machining the specimens. Also, thanks to professor Vidar Hansen, who has helped in many occasions in facilitation of making this thesis better. Thanks to Wakshum Mekonnen Tucho for guidance and the operating of oven for heat treatment. This thesis would have been hard to complete with this level of quality without the help and advice from both lab engineers, professors.

Abbreviations

BCC	Body Centered Cubic
CE	Counter Electrode
CP	Cathodic Protection
IHE	Induced Hydrogen Embrittlement
HEDE	Hydrogen-Enhanced Decohesion
HELP	Hydrogen-Enhanced Localised Plasticity
HESIV	Hydrogen-Enhanced Stress-Induced Vacancy
HISC	Hydrogen Induced Stress Cracking
HV	Hardness Vickers
RE	Reference Electrode
SCE	Saturated Calomel Electrode
SEM	Scanning Electron Microscope
SSRT	Slow Strain Rate Testing
TDS	thermal desorption spectroscopy

Introduction

Due to the world economic recovery and the growing scale of economic development of developing country. The growth and demand of high strength steel is in extreme tension all over the world which is widely applicable in construction and automotive sector due to good mechanical properties. As the demand rises, the deterioration of environmental conditions along the high strength steel are expected to have a good mechanical properties [1]. It is used in various areas like construction industry, car components like door beams, side members, body reinforcement etc. and their application is continuously expanding. High strength steel (X80) is used for transporting natural gas since German Mannesmann Pipe steel company first successfully developed pipeline of 3.2 km test line. In 1992 and 1993 the company developed another pipeline construction for the transportation of natural gas using X80 high strength steels with the delivery pressure of 10 MPa. This pipeline is still working well so far. In several study it was found that the car is subjected to high impact load during accident, so it is very necessary to make tough steel to resist such high impact load [2]. There are various factors for reducing toughness of high strength steel component such as hydrogen during service conditions. automotive industries starts to use advance high strength steel for the manufacturing of components. Whenever High strength steel exposed under the hydrogen environment it could suffer from hydrogen damage or mechanical degradation. This penetrated hydrogen atoms get diffused into the steel and are trapped at dislocations, grain boundaries and other mechanical defects. This individual hydrogen atoms recombine to form a hydrogen molecule and creates pressure on the metal which leads to reduce ductility and cracks starts to begin [3].

Numerous studies focused on the hydrogen influence on the mechanical properties of high strength steel. M. Wang (5) clarified that the tensile strength of both a plain and notched specimen of 1,450 MPa class AISI4135 steel decreased with the hydrogen content due to hydrogen electric charge. Y.D. Li et al.(6) also reported that the fatigue strength of the long-life region of high strength spring steel decreases due to hydrogen content at high temperature and pressure. Depover and Verbeken investigated the effect of HE characteristics in Fe-C-Ti alloys. They found ductility losses due to more trapping capacity of hydrogen in TiC. As the trapping sites increases, the hydrogen diffusion coefficient of alloys decreases [4]. The susceptibility of steel to hydrogen degradation is affect by microstructure and strength level of steel. Steel which have tensile strength of 700 Mpa appear to be resistant of hydrogen cracking and it can be used in various structures without any serious problems. Steel having tensile strength of 1000 Mpa are susceptible to hydrogen induced cracking , and Steel with 1200 Mpa undergo failure with stress below the yield strength. Huang et al. studied the effects of

microstructure and inclusions on the hydrogen induced crack susceptibility of different pipeline steel and concluded that the larger amount of inclusions leads to hydrogen cracking [4].

Hydrogen embrittlement is one of the important factors for the cracking induced in high strength steel. Hydrogen degradation may occur due to the service of construction in corrosive environment causes hydrogen embrittlement, hydrogen induced cracking, or corrosion fatigue. Entering of hydrogen in high strength steel are currently under intensive research and several high strength steel were observed under optical microscope or scanning electron microscope which shows the failure in the regime of about 10^5 to 10^9 cycles in laboratory air.

Even small content of hydrogen are capable to reduce ductility with little change in yield strength as well as tensile strength. The main reason for reducing mechanical properties and sub critical crack growth is absorbed hydrogen [5]. Mainly hydrogen embrittlement are of two types Internal hydrogen embrittlement (IHE) and Environmental hydrogen embrittlement (EHE). In IHE, hydrogen get diffused inside the base material like in steel making process or during fabrication process while in EHE hydrogen enters on the surface of the base material there are various types of environmental assisted cracking are as follows.

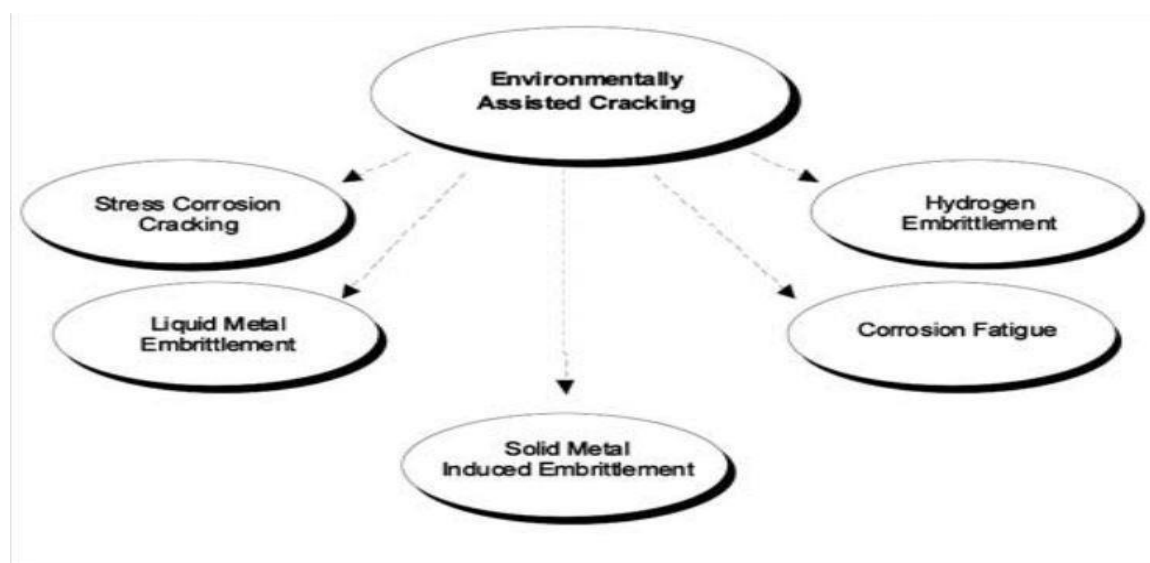


Figure 1 Types of Environmental Assisted Cracking [7]

High strength steel provides proper balance between weight and strength of the components that's why its application is expanding day by day. Hydrogen embrittlement susceptibility can be assessed by slow strain rate test (SSRT) and linearly increasing stress test (LIST). By microstructure examination we can know the effect and consequences of hydrogen. In SSRT

test, applied stress gradually increases and hydrogen simultaneously accumulates in the stress field. Before performing SSRT test, hydrogen is diffused into the material by electroplating, cathodic charging, and welding process. It was found that current density plays important role for the diffusion of hydrogen in high strength steel. The entire hydrogen concentration in the specimen can be measured by thermal desorption spectroscopy (TDS) and the fatigue strength and the tensile strength are degraded []. For example, The content of hydrogen changes in the specimen with time due to hydrogen pressure and temperature. If the current density is high then the more hydrogen diffused inside the base material. Diffusible hydrogen is responsible for the loss of ductility in HSS during straining caused by hydrogen accumulation near dislocations sites and micro voids. Presence of carbides is also responsible for hydrogen related failure. It was found that the size and type of carbides formation plays vital role in trapping capacity of hydrogen.

High strength welded steel is widely used in construction with large scale welded structures due to good strength with high toughness, but also their good weldability. High strength steel are suitable for civil engineering, mining and dredging equipment, bridges, heavy trucks, mobile cranes, pressure vessel pipelines etc. High strength alloy steel is produced directly by quenched and tempered (Thermo mechanical controlled process).

This paper proposes a clear framework of hydrogen impact on the mechanical properties of high strength steel. Furthermore, clear figures and tables are added to assess the diffusion of hydrogen in the specimen and also carried out experimental method. A literature review is done to highlight the diffusion of hydrogen in different types of steel and their impact on the properties. Then, a proposed framework is presented in detail.

1. Theoretical Background

1.1 Overview of the Chapter

The subchapters below explain the behavior of hydrogen diffusion in metals and different factors. This is important information which needs to be understood to fully comprehend the later chapters in the thesis. Fundamental theory is laid forward about general information about the hydrogen embrittlement and their types, later on experimental work is performed to know the mechanical properties of high strength steel.

1.2 Diffusion of hydrogen

Metals often comes contact with hydrogen in environmental conditions. Whenever hydrogen diffuses into the metal it changes the properties of metals. So it is very important to learn behavior of metals which helps engineers to study more about mechanical degradation causes due to hydrogen embrittlement. The diffusivity of hydrogen affects the crack propagation rate and hydrogen absorption influence the rate of hydrogen entering into the steel. There are several ways of diffusing hydrogen inside the metals hydrogen adsorption and hydrogen absorption.

Hydrogen adsorption takes place due to surface imperfections and it gets trapped and immobilizing the atoms. As the series of defect or imperfection surface rises the more hydrogen atom attracts towards the surface. The ionization of gas atoms takes place and form a new phase of hydrides. Diffused hydrogen atoms desorbed the metal surface and these desorbed atoms recombine to form hydrogen molecule- There are various methods though which hydrogen adsorption is present like electrochemical charge, atmosphere loads of hydrogen gas and the surface conditions (1). Diffusion of hydrogen in steel takes place at interstitial sites where the octahedral sites occupies a higher temperature while tetrahedral sites occupied low temperature (4), which increases kinetic energy and mobilization of atoms into the metal matrix with the increase in temperature. The hydrogen absorption techniques can be described by following equations.

$$D = D_0 e^{-EA/(kT)} \quad (1)$$

Where, D=diffusion coefficient (m^2 / s),

D_0 =Maximum diffusion coefficient (at absolute temperature; m^2/s),

EA=Activation energy for diffusion with dimensions of ($J \text{ atom}^{-1}$),

T=absolute temperature (K), k is the Boltzmann constant.

The absorption can be explain in two mechanism, classical mechanism of absorption in a molecular form and Crolet ion mechanism. The equation for the mechanism are as follows



$$I_{abs} = K_{ab} \theta \left(1 - \frac{N_0}{N_s} \right) - k_{des} C_0 (1 - \theta) \quad (3)$$

Where, I_{abs} = Reaction's Rate, K_{abs} =Absorption Rate, K_{des} =Desorption Rate, C_0 = hydrogen concentration in metallic layer, $(1-\theta)$ = No of active sites on the surface. The first equation is for absorbed elements and the second equation in about desorption [12].

Change of atoms is another method for the insertion of hydrogen in metallic elements where the hydrogen atoms substitute metal atoms increases the embrittlement of material and the mobility one layer over the others decreases. As shown in figure In the rising part the traps are filled and steady state corresponds to diffusion in the lattice with saturation of the traps where some of which are exchanging hydrogen with lattice (Reversible Traps). The deeper traps are not interacting with hydrogen diffusion. Once the steady state achieved, cathodic charging interrupted and anodic current value decreases.

1.2.1 Hydrogen Enhanced Decohesion Mechanism

Troiano developed the HEDE mechanism in 1959, in which he explained how the presence of a hydrogen atom at the fracture tip reduces interatomic strength and causes brittle failure. This occurs due to the material's surface energy, and the fracture occurs below its working stress. If the specimen is exposed to a hydrogen atmosphere with many hydrogen atoms, the atom on the first cell reaches the 3d cell of the iron atom, causing fracture at low working stress. Internal hydrogen embrittlement and exterior hydrogen embrittlement are both addressed by the HEDE mechanism [8]. Due to adsorbed hydrogen, atoms decohesion happens most commonly at the crack tip and the place of maximal hydrostatic stress. , It also happens at particle matrix contacts. Decohesion may occur if hydrogen accumulates in the grain boundary near the crack tip and is trapped in a specific area due to the influence of hydrogen and impurities inside the metal matrix [9].

1.2.2 Hydrogen Enhanced local plasticity

In this mechanism, hydrogen atoms gathered in the fracture tip zone, lowering the resistance to dislocation motion. As a result, dislocation mobility increased, acting as plastic deformation carriers in the metal lattice. Due to local drop-in yield stress, local dislocation movement is feasible at low levels of stress. This means that embrittled material exhibits local plastic deformation at the fracture surface and slip bands at the crack tip zone. However, the relationship between the intended and proposed HELP model and the actual embrittlement mechanism remains unclear. Microstructure investigation has shown fracture modes such as intergranular, transgranular, and quasi-cleavage and it mainly depends on the hydrogen content in the surrounding (hydrogen atmosphere) and crack tip stress intensity [10]. Brittle fractures are commonly associated with hydrogen-related fractures. However, a detailed fractographic inspection will reveal a plasticity near the crack tip.

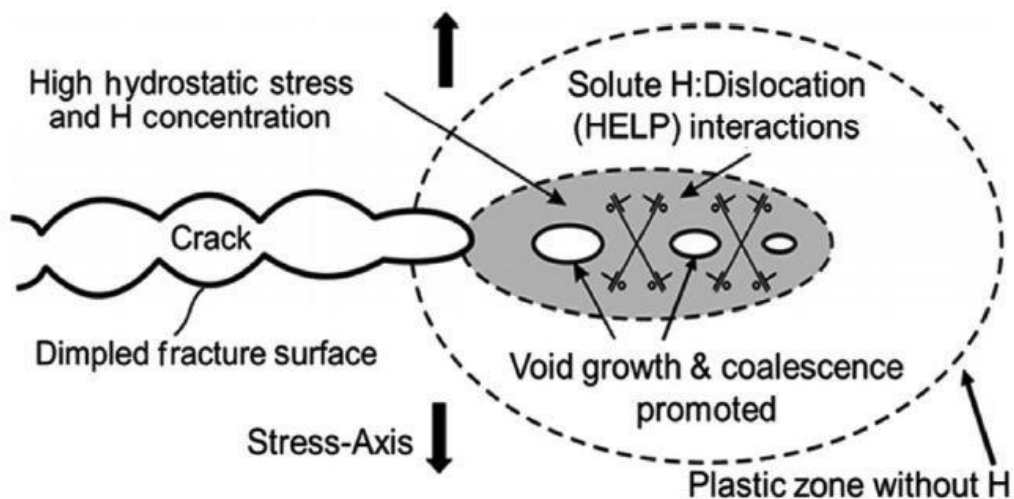


Figure 2 Hydrogen Enhanced local plasticity [10]

1.2.3 Hydrogen Enhanced Macroscopic Ductility (HEMP)

Due to hydrogen diffusion and solid solution softening by the hydrogen atom, the mechanical characteristics of materials alter and yield strength of materials is reduced when the specimen is surrounded by a hydrogen environment. Hydrogen Enhanced Macroscopic Ductility is demonstrated by the drop in yield strength caused by the presence of hydrogen (HEMP). Because of the presence of hydrogen in the environment, there is a possibility of increased dislocation motion, as well as continued plastic deformation at a lower functional stress rate. The main cause of the material's ductility degradation and shift in fracture mode from cup and cone to brittle shear at ultimate tensile strength is hydrogen charge[11].

1.3 Effect of hydrogen on the mechanical properties of steel

There is a great impact of hydrogen and hydrogen environment on the mechanical properties of steel. The specimen is loaded uniaxial tension until failure where the specimen can be smooth bar, notched bar or a plain strain specimen. The tensile test of specimen helps to identify the yield strength, ultimate strength, total elongation and reduction in cross section area. Two approaches have been developed for tensile test 1) Slow strain rate test (SSRT) which increases strain until fracture. 2) Linearly increasing stress test which increases stress until fracture [10].

1.4 Ductility

Several test has been performed which showed that for the ferritic-martensitic steel T91, the elongation and the reduction of area decreased due to hydrogen charging (Tests by Marchetti, Herms, Laghoutaris, and Chêne (2011)). Ludwik [13] found considerable changes both in elongation and, particularly, in the reduction of fracture values in mild steel specimens after pickling in 2.5% sulphuric acid. Bastien and Amiot , Amiot and Skluev et al. concluded that the higher the tensile strength Bastien and Amiot (1954), Amiot and Skluev et al. concluded that the higher the tensile strength more the degree of embrittlement. But if the equal tensile strength values are there, different susceptibilities were observed, depending on the structure of the steel. Also, Steels with lower susceptibility have higher ductility, and their actual states are closer to those of physical-chemical, structural, and mechanical equilibrium. Heat treatment is the process of heating and cooling metals to get the desired properties of metals at a specific temperature. Different ways for a better heat treatment procedure have been developed over time. Heat treatment is used for a variety of reasons, including making metal soft [9] and increasing hardness. This also improves the metals' electrical and thermal conductivity.

1.5 Heat Treatment

Heat treatment is a process of heating and cooling the metals at certain temperature to obtain the desired properties of metals. Over a time different methods has been developed for the better heat treatment process. There are various reasons for carrying out heat treatment process like to make metal soft , while other increase hardness. This also increase the electrical and heat conductivity of the metals. Some metals goes through different heat treatment process as per the applications. In simple terms, It is a process to heat metals at certain temperature, hold it for some time and then cooling it back. This process change the microstructure and mechanical properties of metals. Outcome of the process is fully depend on the time duration of heating, time of keeping metal at certain temperature, rate of cooling, surrounding conditions, coolant etc.

It also depends on the metal type, size and heat treatment process. Over the course of this process, the metal's properties will change. Among those properties are electrical resistance, magnetism, hardness, toughness, ductility, brittleness and corrosion resistance. Heat treatment is mainly done according to iron carbon diagram as shown in the figure. This shows a structural changes that takes place at different temperature. The iron carbon diagram is very important to know the changes in the metals when subjected to heat treatment. The X axis shows the carbon content in the alloy where y axis shows temperature. As shown in the figure there are different regions where the metal exists in different microstates such as austenite, cementite, and pearlite. The phase of the metal changes when it is passes through that temperature or carbon content. The phase diagram is an crucial tool to identify whether heat treatment will be beneficial or not. Each structure brings along certain qualities to the final product and the choice of heat treatment is made based on that. The most common method used in hardening is annealing, Normalizing, hardening, Ageing, Stress relieving, Tempering, Carburization.

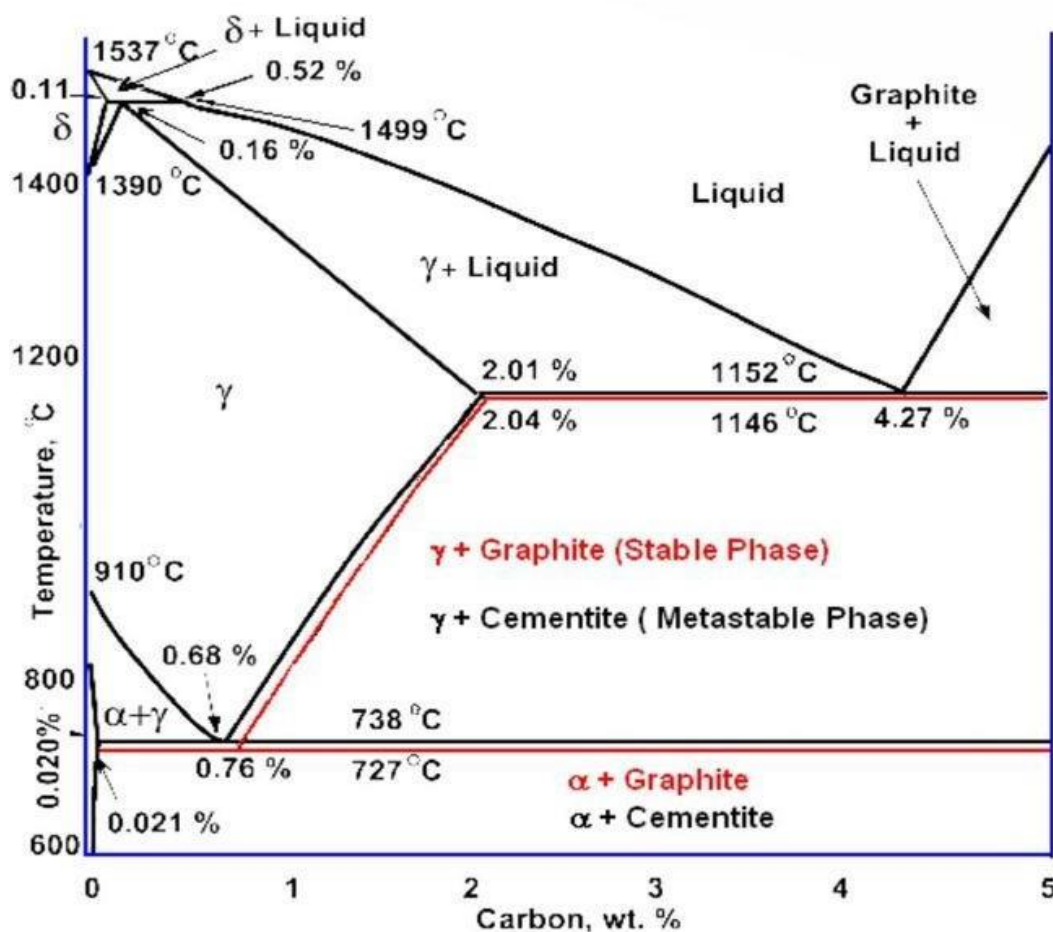


Figure 3 Iron carbon Phase Diagram [4]

When a metal is hardened, it is heated to a certain temperature well above the austenite transformation temperature. After that, it's quenched (quickly cooled) in water or oil, resulting

in martensite. A fast cooling rate is needed because a slow cooling rate can cause the metal to turn into pearlite or bainite. A body-centered tetragonal unit cell (BCT) is found in martensite. For a given iron-carbon alloy, a TTT-diagram (Time, Temperature, and Transformation) will show the basic principles of the process. TTT-diagrams vary depending on the alloy, but the basic idea remains the same. The transformation of austenite to martensite starts when the metal reaches a critical lower temperature. Each atom is slightly displaced relative to its neighbors during the martensitic transformation. This results in the polymorphic transformation of the austenitic face centered cubic (FCC) structure to the martensitic BCT-structure. The carbon atoms are trapped in the lattice during this process, working against dislocation motions. The amount of carbon in a martensite determines its hardness, which is equal to the carbon in a carbon-manganese steel [2]. HISC is more common in untempered martensite [10].

1.6 Tempering

Tempering is a process to increase the hardness of iron based alloys. Tempering can be achieved by heating the samples below the critical temperature for a period of time, then cooling it in air. The amount of hardness extracted is determined by the exact temperature, which is dependent on both the alloy's composition and the desired properties in the finished product. Extremely hard tools, for example, are often tempered at very low temperatures, while springs are tempered at much higher temperatures. Tempering steel after it has been hardened achieves a balance between hardness and strength. Allowing carbon diffusion to occur within a steel microstructure achieves this. Steel can become overly brittle and hard when it is hardened. The steel, however, does not have the strength or abrasion resistance needed for its intended application if it is not hardened. Tempering a hardened steel also increases its machinability and formability, as well as lowering the risk of it cracking or failing due to internal stresses. Following a quenching process, tempering is most widely used. When a carbon steel is heated and quenched quickly, it can become too hard and brittle. It can be tempered to regain some of its ductility. Tempering a welded part will reduce its hardness and alleviate stress. Welds can harden a localized zone due to the heat generated during the welding process. This can result in unfavorable mechanical properties and residual stress that may contribute to hydrogen cracking. Tempering is a good way to avoid this [20]. Tempering is often needed for work-hardened materials. Punching, bending, shaping, drilling, and rolling are all examples of work hardening processes. Relatively high residual stresses exist in work hardened materials, which can be reduced by tempering.

1.7 Vickers Hardness Test

During their time at Vickers Ltd, Robert L. Smith and George E. Sandland invented this technique in 1921. It was created as a replacement for the well-known Brinell hardness measure, but it uses a simplified scale. Metals and other similarly hard materials may be tested using the Vickers technique. It was, however, mainly created to concentrate on softer materials, such as plastic, and their ability to resist deformation under constant stress. The Vickers procedure, like many other hardness tests, uses its own unit of hardness. The Vickers test technique involves dropping a load into an indenter, which leaves a mark on the material's surface, much like every other hardness test. However, the sample must have a flat surface in order for the findings to be correct. This implies that the sample must be polished to fulfill the test's requirements. When the material is ready, it will be put on the tester, where it will come into contact with the indenter.

Vickers Hardness test blocks may also be used to correctly calibrate the tester for the operation. Vickers Indenters have the same size and composition across all studies, which is a unique function. In fact, only one type of indenter is used in the Vickers procedure: a diamond shaped like an inverted pyramid (hence it being called the Vickers Pyramid). The reasoning behind this is that in order for the findings to be measurable, the impression to be left on the substance must have a well-defined form. In addition, the indenter itself should be made of a deformation-resistant material [11]. Diamonds are an excellent match for this requirement. The load is lowered after the tester has been balanced, causing the indenter to pass through the material's surface. As gravity tends to force the indenter deeper into the material, it will stay there for a long time (also known as dwell time). Once the dwell time has elapsed, the load is removed and the indenter is released [19]. The operator is then tasked to perform optical evaluation wherein they will examine the dimensions of the indentation left and use a specific equation to come up with the material's hardness value.

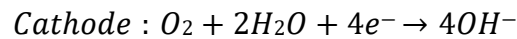
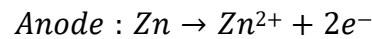
1.8 Tensile Testing

The strain rate is important when conducting a tensile test with hydrogen, whether the specimen is precharged or under CP. Hydrogen must have time to disperse in order for the mechanism to work. As a result, the strain rate must be slow enough for the cracking to spread in a stepwise manner. Mainly tensile test is carrying out with specimen having smooth parallel surfaces. However hydrogen can only diffuse in elevated hydrostatic stress. In order to create a region of increased tri-axial stress in a smooth specimen, the specimen must be necked. The necking zone is above the maximum nominal stress. As a result, there is a smooth transition. The presence of a threshold stress in a specimen cannot be determined. The hardness of the material

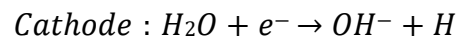
has a major impact on hydrogen embrittlement [13]. For all degrees of stress, a notch in the parallel surface guarantees hydrostatic stress. The maximal local stress can then be modeled using the finite element method to determine a theoretical threshold stress. By comparing the nominal fracture stress of the hydrogenated specimen to the yield stress in air, this technique is more than elaborate, and very satisfying results can be obtained.

1.9 Cathodic Protection

Cathodic protection is the most effective and extensively utilized tool for preventing corrosion (CP). In subsea conditions, cathodic protection acts as a catalyst for hydrogen diffusion into carbon steels such as AISI 4130. As a result, studying CP's electrochemistry is required to determine the source of hydrogen. The three separate components are the anode, cathode, and electrolyte (or connection to an external power source). Electrons are sent from the anode to the cathode, and cathode receives that electrons. The anode is either a lower-voltage electrode or a lesser noble metal that functions as a sacrificial anode. In a CP arrangement, the anode and cathode can be connected directly or via wire. Faraday's rules of electrolysis confirm the chemical reactions for anode and cathode shown in Figure 3 in the chemical reaction equation below. The cathodic reaction is represented by two equations, each of reaction triggered by the presence of negative potential, as stated in the following text. [12]



or



2. Experimental Work

2.1 Chemical Composition and Cutting Process

The chemical composition of material are as follows.

Table 1 Chemical composition of material

Element	Wt(%)
C	0.75
Si	0.33
Mn	0.75

A Pulous SCK 400 Plus metal band saw was used to cut the specimens along the steel plate of size (500mm*250mm*6mm). We could extract 25 pieces from the metal plate (250mm*20mm*6mm) and this was calculated with the tolerance of ± 2 mm. To facilitate clamping of plate, two flat plate of steel were used which had grooves to fit accurately. Clamping the pipe between these two steel plates ensured that the plate lay stable in the saw. Before each cut was performed the breadth of the work piece was carefully measured and then cross checked.



Figure 4 Rectangular bar to cut pieces



Figure 5 Sample after cutting rectangular plate using band saw machine

2.2 CNC of Samples

The CNC machine was used to cut the shape of samples. It was then programmed to cut the reduce area, and the specimen was put inside the machine to confirm that cut was correct or not. The whole sample cutting was performed after the heat treatment process. The size and shape of tensile tests specimens are as follows. This designed is made as per the ASTM standards.

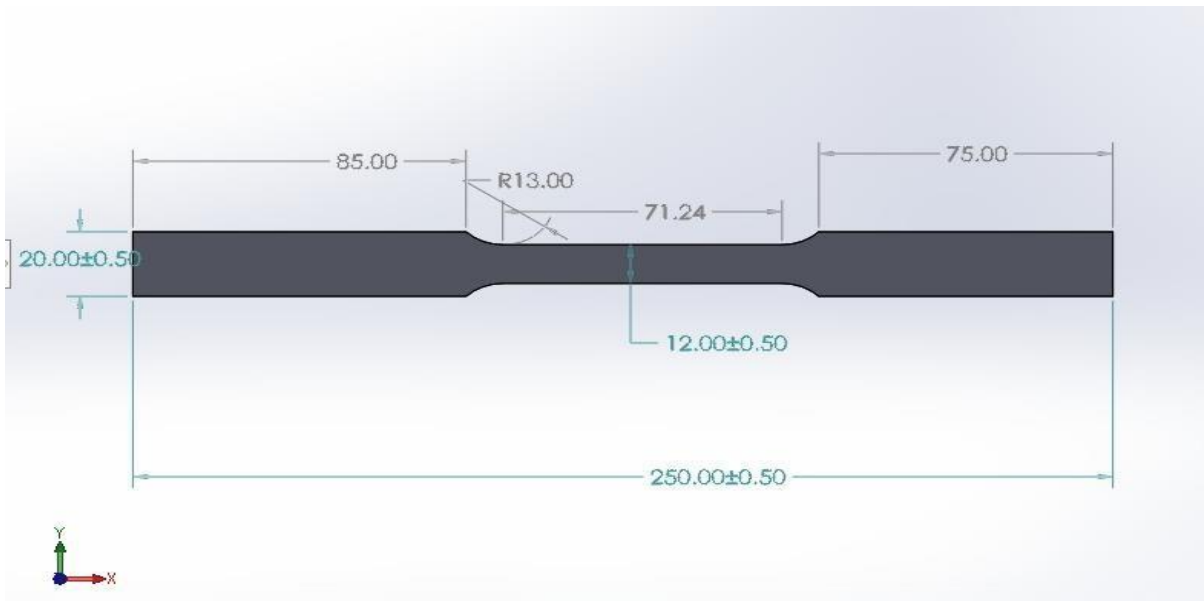


Figure 6 Specimen design as per the ASTM standards



Figure 7 Specimen after CNC machining

2.3 Setting Serials number on Samples

It was very important to label all samples before heat treatment. All samples were similar prior to this phase, but after heat treatment, they would have different hardness values. A three-group system was divided, with each series including different samples. Table shows a summary of the data. The samples are numbered.

Table 2 Serial numbers of different samples

Group 1	Group 2	Group 3
1	1-HC	2-HC
2	3-HC	4-HC
3	5-HC	6-HC
4	8-HC	7-HC
5		
6		
7		
8		
9		

2.4 Heat treatment and Quenching

After cutting and setting serials numbers on the samples, the next step is to increase the hardness of the sample. The oven was set at 900 degree Celsius and settle it for 24 hours where all samples were mounted on single rod and heated at 900 degree Celcius for 30 minutes. After heating the samples it is immediately quenched into the oil for cooling . Firstly all specimens were placed in oven at 900 degree Celsius for 1 hour, the hardness value was less as compared to the duration of 30 minutes. Finally, we decided to go with the 30 minutes duration.

Table 3 Heat treatment of all samples

Number of Samples	Hardening Temperature	Time Interval
15	900°C	30 Minutes



Figure 8 Samples in oven for heat treatment process



Figure 9 Quenching of samples after heat treatment process

2.5 Hardness test after hardening the samples

After performing heat treatment process, it is essential to check hardness of the samples so that we can confirm whether desired hardness was obtained or not. A small piece of sample cut (20mm) from the end of the piece using Struers Discotom. This sample was then polished and subjected to a Vickers hardness test. A VH of 235-244 was determined by indenting every 1 mm along the surface area of the cross-sectional region, showing that the steel had been properly hardened.

2.6 Tempering

The tempering process of all specimens was done in an interval between 350°C to 550°C to reduce the level of hardness value. Different samples of different series group were heated at 350°C, 450°C and 550°C. Following tables shows description of all tempered samples.

Table 4 Tempering of Group 1

Serial Number	Temperature °C	Time
1	Raw Sample	-
2	Raw Sample	-
3	As Quenched	-
4	As Quenched	.
5	350	60 minutes
6	450	60 minutes
7	450	60 minutes
8	550	60 minutes
9	550	60 minutes

Table 5 Tempering of Group 2

Serial Number	Temperature °C	Time
1-HC	350	60 minutes
3-HC	450	60 minutes
5-HC	550	60 minutes
8-HC	As Quenched	-

Table 6 Tempering of Group 3

Serial Number	Temperature °C	Time
2-HC	350	60 minutes
4-HC	450	60 minutes
6-HC	550	60 minutes
7-HC	As Quenched	-

2.7 Sample preparation for hardness test

A length of 10 mm was cut from each sample with Struers Discotom machine to measure hardness of each sample. All pieces were marked with serial number to avoid confusion between the pieces. These samples were molded in resin and then polished with 80, 500 and 2000 grit paper with diamond paste. Samples were washed after each cycle before being dried with air, it was washed with deionized water and ethanol.



Figure 10 Plastic molded for hardness test

2.8 Electrolysis

As an electrolyte, a 20L square plastic container with a capacity of 8 samples was filled with 3.5 wt % NaCl in distilled water. The NaCl electrolyte was chosen specifically to mimic the marine environment. The pre-charging setup included an AISI 1074 sample as the working electrode and a titanium bar as a counter electrode. In this process 3.5%wt of NaCl was used for the ionization of distilled water. On Anode, Titanium bar is used, Cl⁻ oxidized and bonded Cl₂. Where H⁺ ion reduce and form atomic and molecular hydrogen. A three electrode were used to achieve a desired potential level of (-1110 mV). Titanium plate are considered as counter electrode with standard calomel reference electrode and a voltmeter. The voltage source were supplied to the electrode where ampere is used to determine current in working\counter electrode circuit.

Two groups of hydrogen charged samples were charged for approximately 2 weeks prior SSRT. The hydrogen charged was started at same time for all the samples. The fully saturation of

hydrogen can be achieved for all the AISI 1074 samples during approximately 2 weeks. The test samples would be saturated with hydrogen during this incubation period.

Table 7 Hydrogen charge duration of all samples

Sample Designation	Tempering Temperature	Hydrogen Charging Duration
1	Raw Sample	0
2	Raw Sample	0
3	As Quenched	0
4	As Quenched	0
5	350	0
6	450	0
7	450	0
8	550	0
9	550	0
1-HC	350	290
3-HC	450	316
5-HC	550	329
8-HC	As Quenched	341
2-HC	350	314
4-HC	450	331
6-HC	550	339
7-HC	As Quenched	357

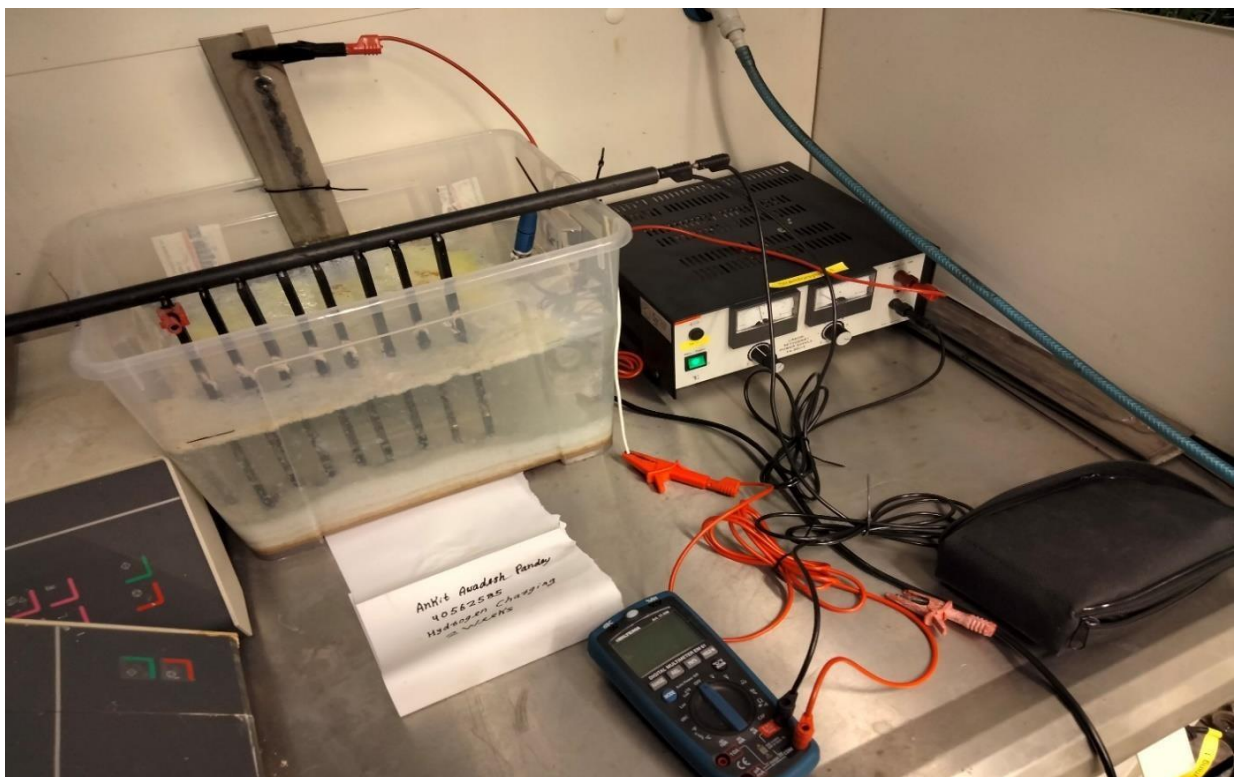


Figure 11 Electrolysis process for hydrogen charging of all samples

2.9 Tensile test under cathodic protection

A plastic container of diameter 55mm and height of 100mm are used as the container for the experimental process. The container is fully filled with the distilled water with 3.5% wt of NaCl such that the sample gets fully submerged in water and SCE were sufficiently submerged. The water was changed after certain period of time to ensure a constant environment. The following component were used for the final set up A) Saturated calomel electrode B) Voltmeter C) Adjustable resistor D) Adjustable DC Power supply E) Sea water and box F) Rod as cathode and test samples. A three electrode system was used to do hydrogen charging for the samples. All the samples were charged potentiostatically under a tensile load. The three electrode used were titanium as a counter electrode, and saturated calomel electrode as a reference electrode. The potential was set at 1100 mV Gamry interface. All the samples mounted on the tensile machine for the testing at different strain rates. The hydrogen charged samples transferred from incubation container to tensile test cell within 5 minutes to minimize the losses of hydrogen from the samples. It is very crucial to test all the samples at unique strain rate while the uncharged samples were tested in air (Open Environment). Uncharged samples were tested at the same strain rate, load vs displacement data were recorded for all the samples.

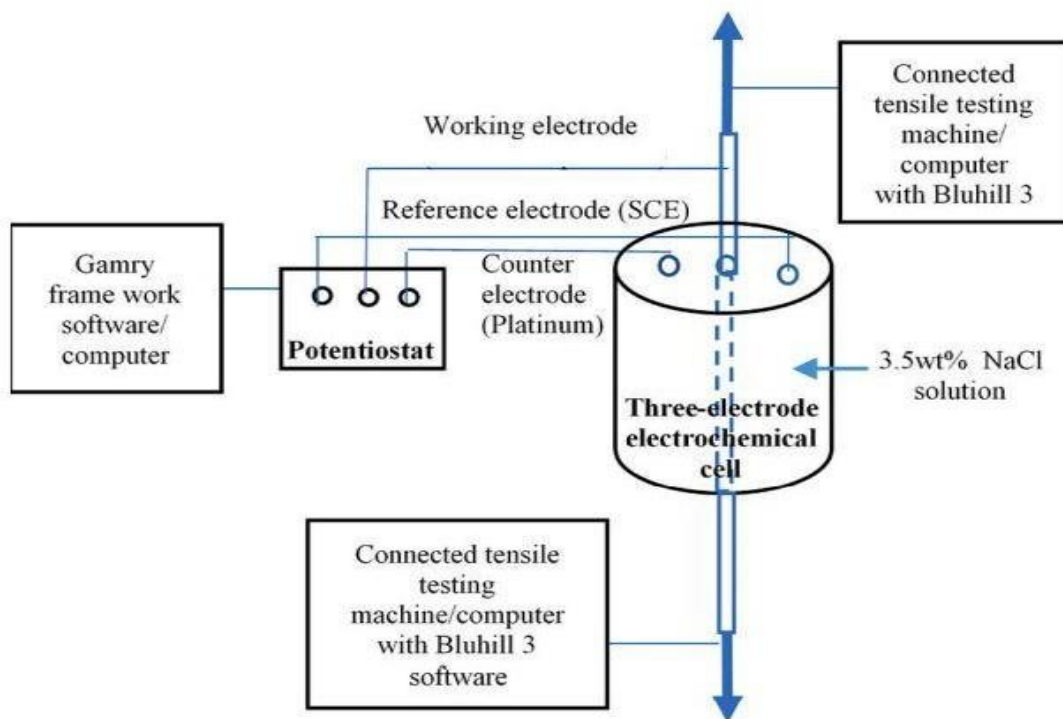


Figure 12 Schematic diagram for tensile test [13]

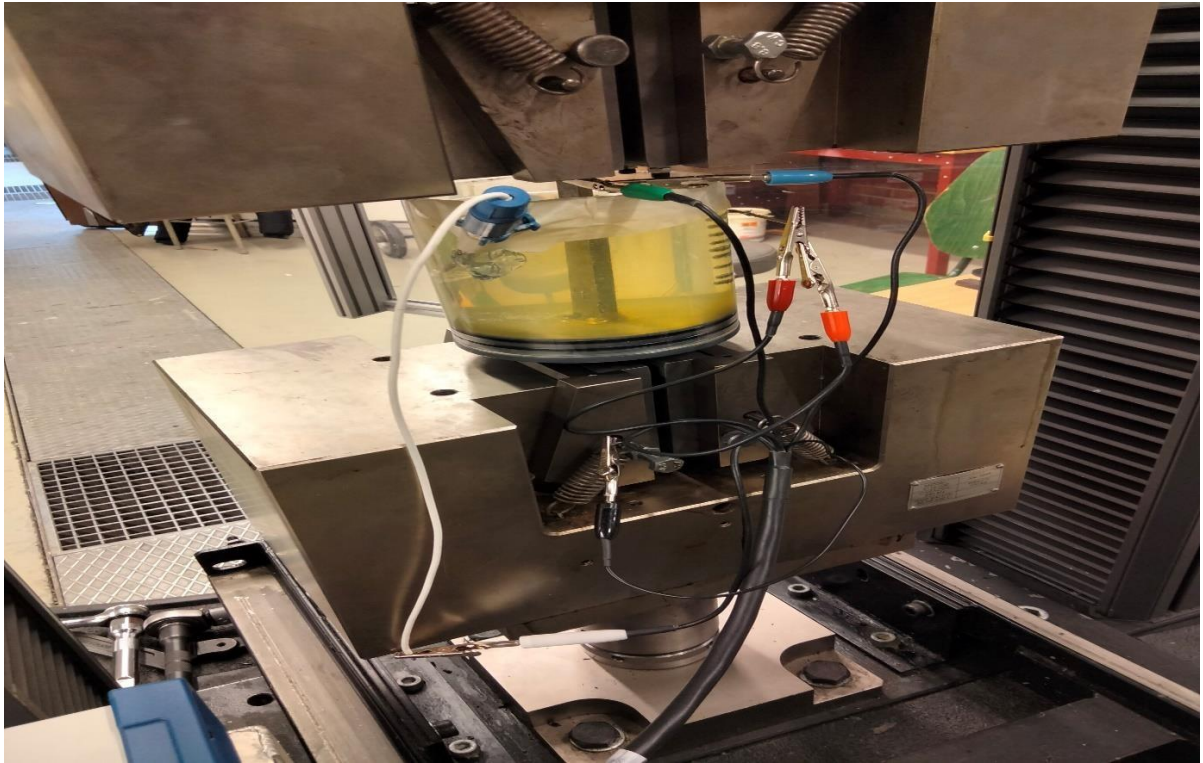


Figure 13 Set up for tensile testing

The cross sectional area is reduced during tensile test and total elongation length were measured after the fracture of samples. The relative HE susceptibility I_{HE} is defined by the ratios of stress-strain curve characteristic parameters of samples tested after hydrogen charging using the characteristic parameters of the samples tested in air. A slow strain rate is applied to specimen for migration of hydrogen to crack tip during propagation. There is a effect of strain rate in the percentage of the reduction area, due to this all the hydrogen charged samples were tested at different strain rate. The tensile test for uncharged specimen is done in air. After performing tensile test the cross sectional area reduced and total elongated length of specimen were measured.

3. Results

3.1 Vickers Hardness Testing

A struers durascan was used for the hardness testing of different tempered sample. Numbers of indentations were made to each sample using the HV10 method. The results are summarised in Table 7 below, where the arithmetic mean value of the hardness testing is displayed, along with the associated standard deviation. The temperature at which each sample was tempered is also displayed. All samples were tempered for 60 minutes, apart from the as quenched samples and raw samples.

Table 8 Hardness value of all samples

Sample Designation	Tempering Temperature	Hardness (HV)
Sample 1	Raw Sample	239±4
Sample 2	Raw Sample	234±6
Sample 3	Hardened	667±5
Sample 4	Hardened	646±3
Sample 5	Hardened-Tempered 350	587±8
Sample 6	Hardened-Tempered 450	492±12
Sample 7	Hardened-Tempered 450	498±7
Sample 8	Hardened-Tempered 550	389±3
Sample 9	Hardened-Tempered 550	386±2
Sample 1-HC	Hardened-Tempered350-Charged	595±5
Sample 2-HC	Hardened-Tempered350-Charged	594±4
Sample 3-HC	Hardened-Tempered450-Charged	491±9
Sample 4-HC	Hardened-Tempered450-Charged	493±6
Sample 5-HC	Hardened-Tempered550-Charged	389±4
Sample 6-HC	Hardened-Tempered550-Charged	391±2
Sample 7-HC	Hardened-Charged	673±4
Sample 8-HC	Hardened-Charged	671±6

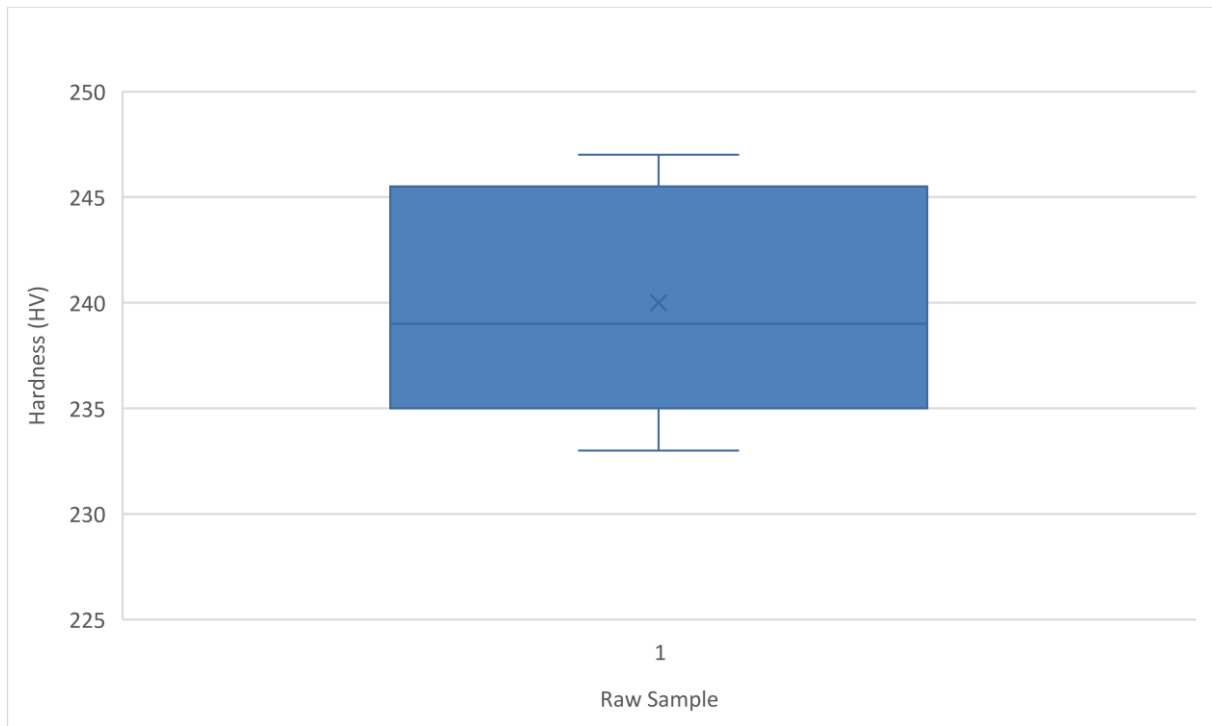


Figure 14 Hardness graph of raw sample

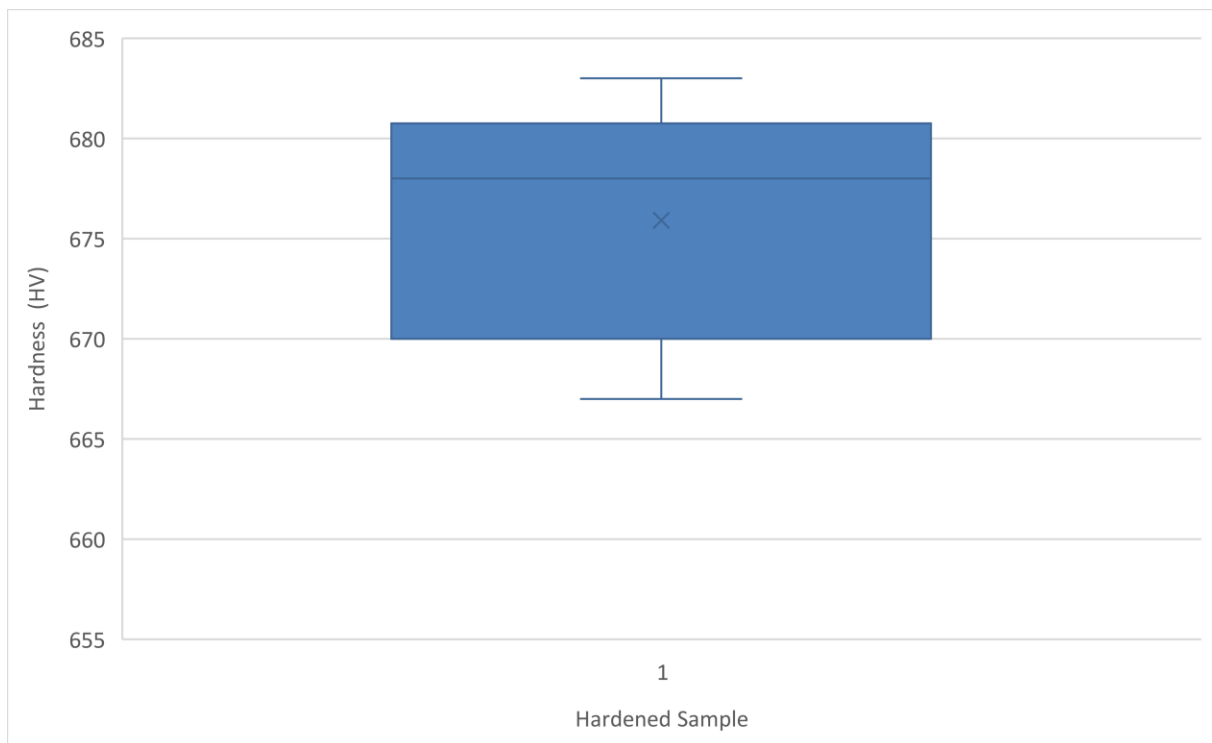


Figure 15 Hardness graph of hardened sample

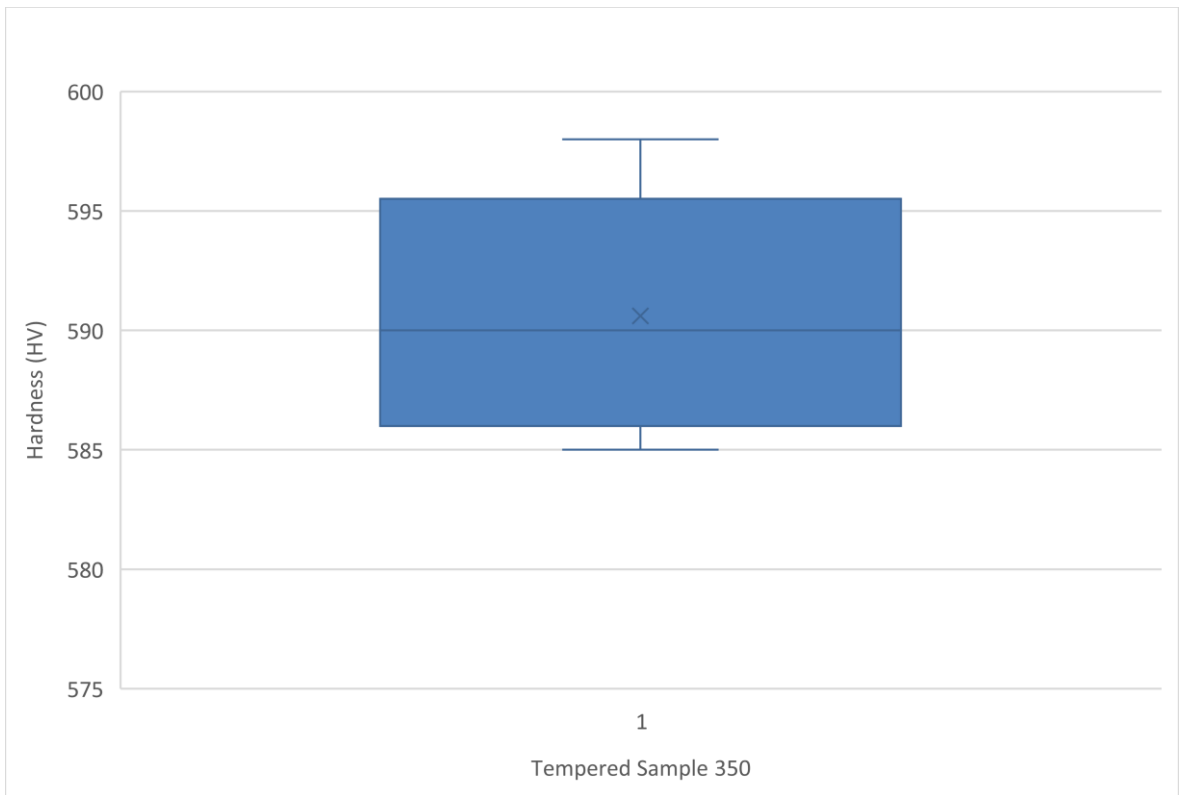


Figure 16 Hardness graph of tempered sample 350

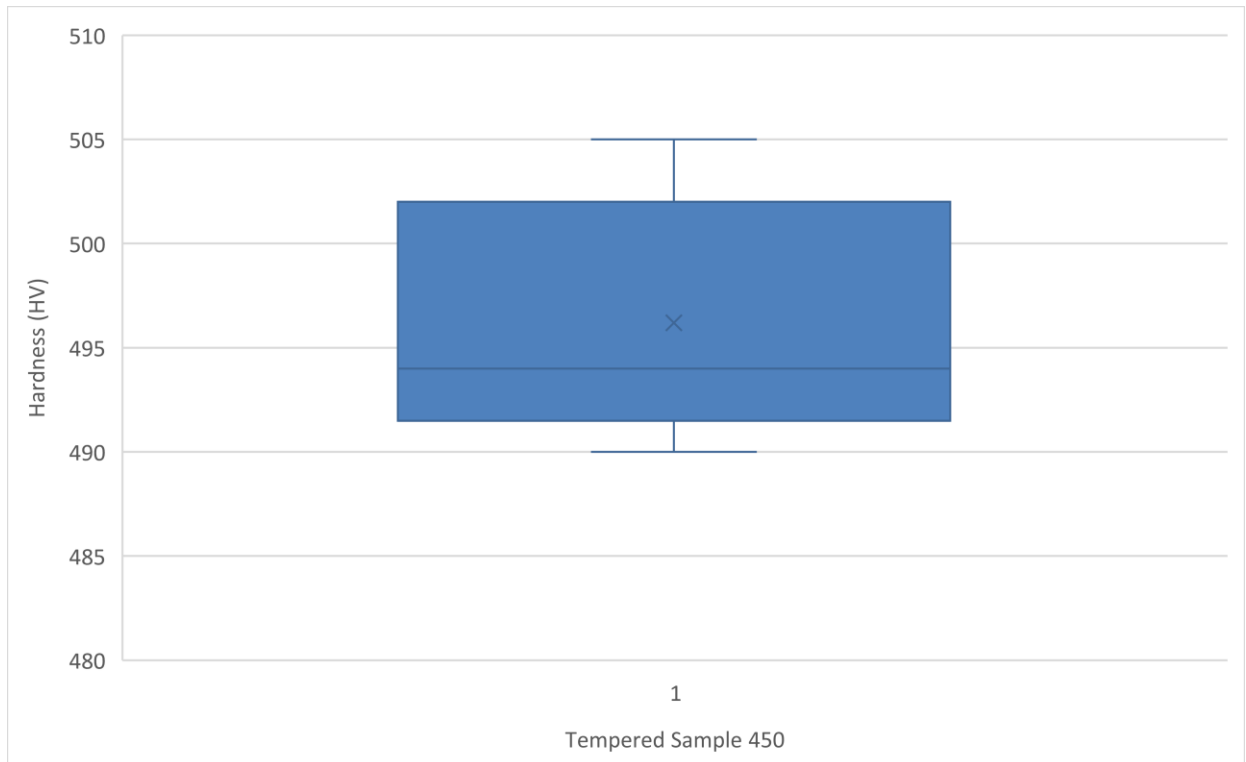


Figure 17 Hardness graph of tempered sample 450

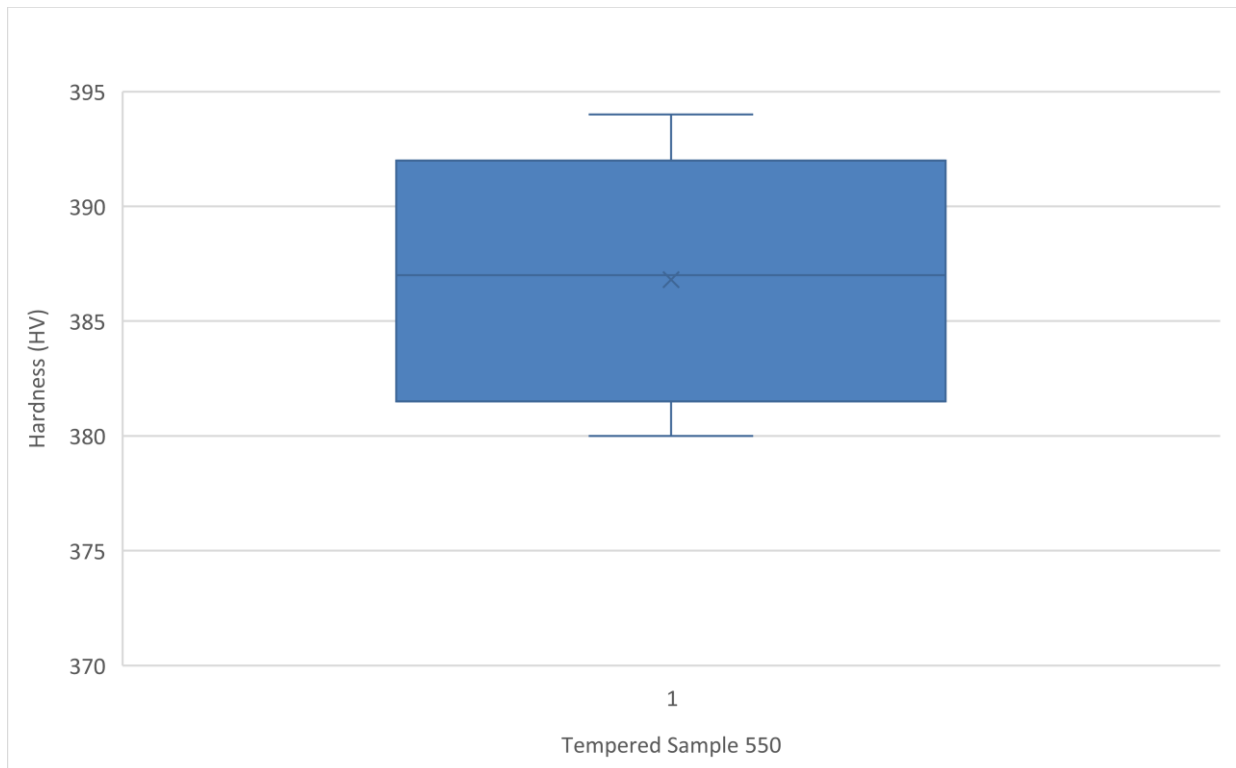


Figure 18 Hardness graph of tempered sample 550

3.2 Tensile test under cathodic protection

The tensile test is performed after two weeks of hydrogen charging as per the procedure mentioned in the experimental work. For getting better understanding of tensile properties it is necessary to have the nominal stress-strain behavior of hydrogen charged and uncharged samples. The results below shows tensile test of different series. 1 Series were tested in air and the last two series were tested in electrolyte.

3.2.1 Tensile Test in Air (Series 1)

It is clearly seen from the graph that the specimen is extended more with the increase in the tempering temperature and yield strength also tends to decrease. Ductility of specimen increases with the tempering temperature. The tensile strength of sample decreases with the increase in the tempering temperature. The area reduction of sample tempered at 350°C and 450°C are nearly same and sample tempered at 550°C has more area reduction.

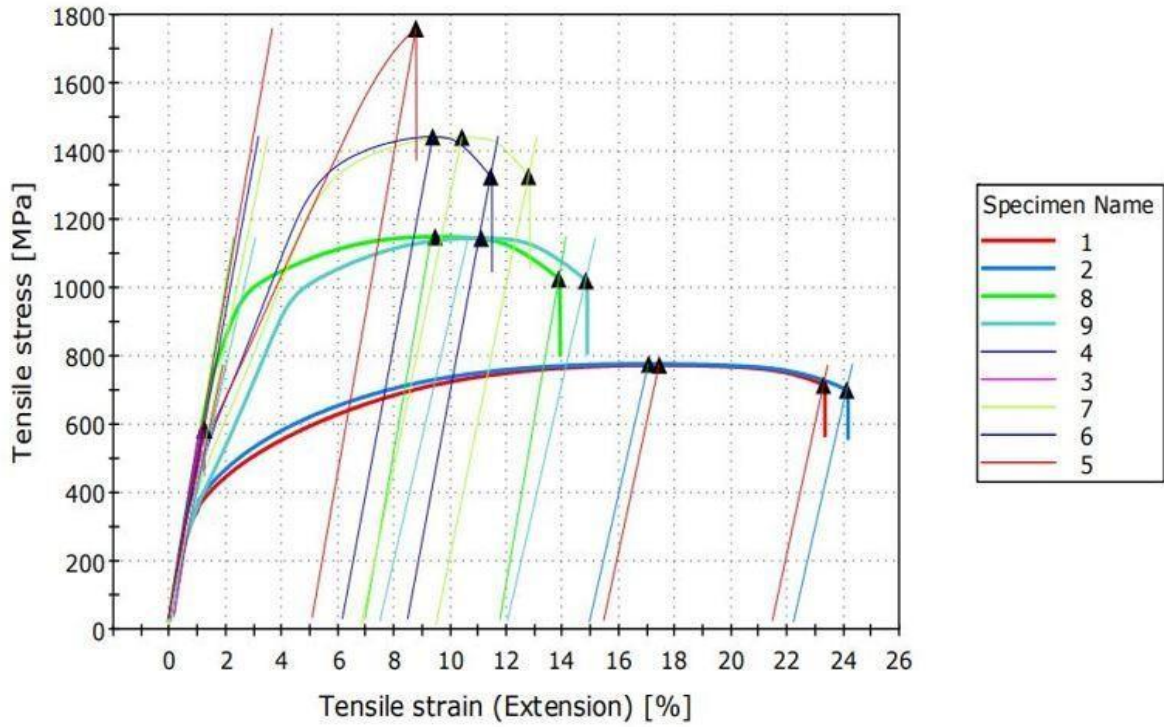


Figure 19 Tensile strength of all raw samples

Table 9 Modulus, Tensile strength, and Area reduction of series I

Serial No.	Temperature	Modulus E	Tensile Strength	Area Reduction in %
1	Raw Sample	38	776	1.054
2	Raw Sample	36	779	2.062
3	Hardened	49.8	588	0.6504
4	Hardened	50.3	587	0.612
5	Hardened-Tempered 350	46.5	1758	6.54
6	Hardened-Tempered 450	43.7	1443	6.46
7	Hardened-Tempered 450	39.8	1441	6.32
8	Hardened-Tempered 550	47.4	1551	9.35
9	Hardened-Tempered 550	35.7	1147	12.35

3.2.2 Tensile test for hydrogen charged Sample (Series 2 and Series 3)

If we compare the samples of hydrogen charged with uncharged samples, there is a large difference in extension and tensile strength of the materials. The duration of hydrogen charged samples also plays a important role during tensile test. The same general trend was observed in series 1 can also be observed in series 2 and series 3. The tensile strength of sample increases with the increase in the tempering temperature. This charged samples which placed for a longer time have some differences in the tensile strength, and the extension of material as shown in graph and table.

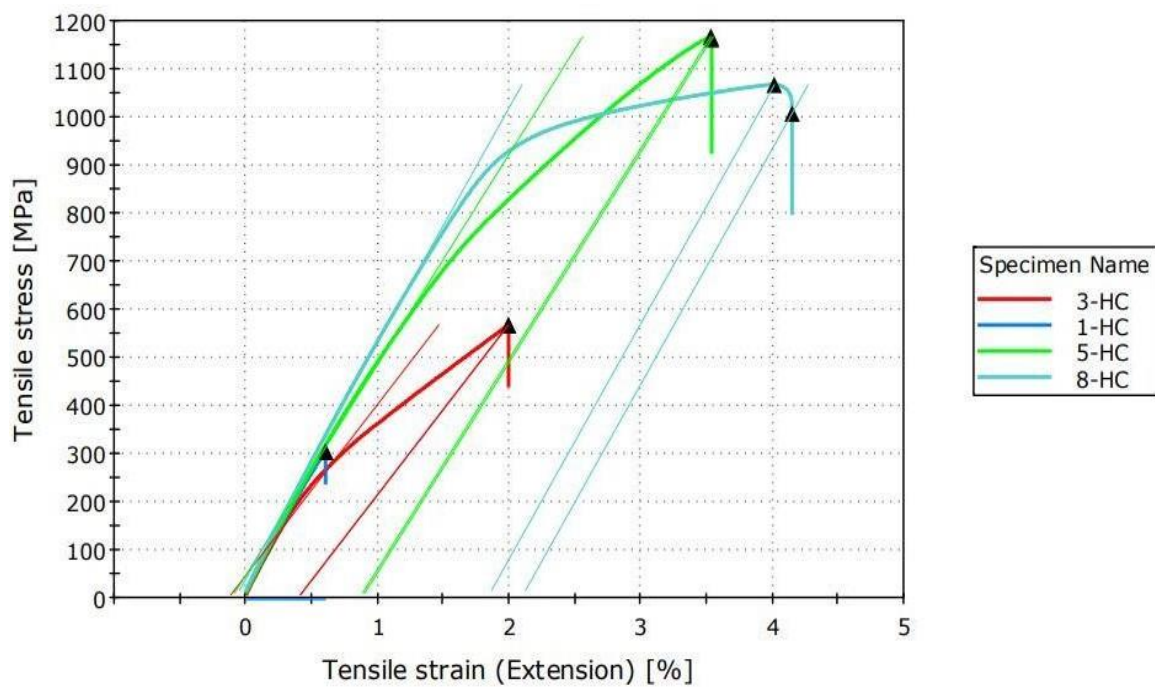


Figure 20 Graph of hydrogen charged sample (Series 2)

Table 10 Tensile strength and Area reduction of series 2

Serial No.	Temperature	Duration (In hrs)	Tensile Strength	Area Reduction
1-HC	Hardened-Tempered350-Charged	290	306	2.2
3-HC	Hardened-Tempered450-Charged	316	568	1.6
5-HC	Hardened-Tempered550-Charged	329	1161	3
8-HC	Hardened-Charged	341	1007	0.71

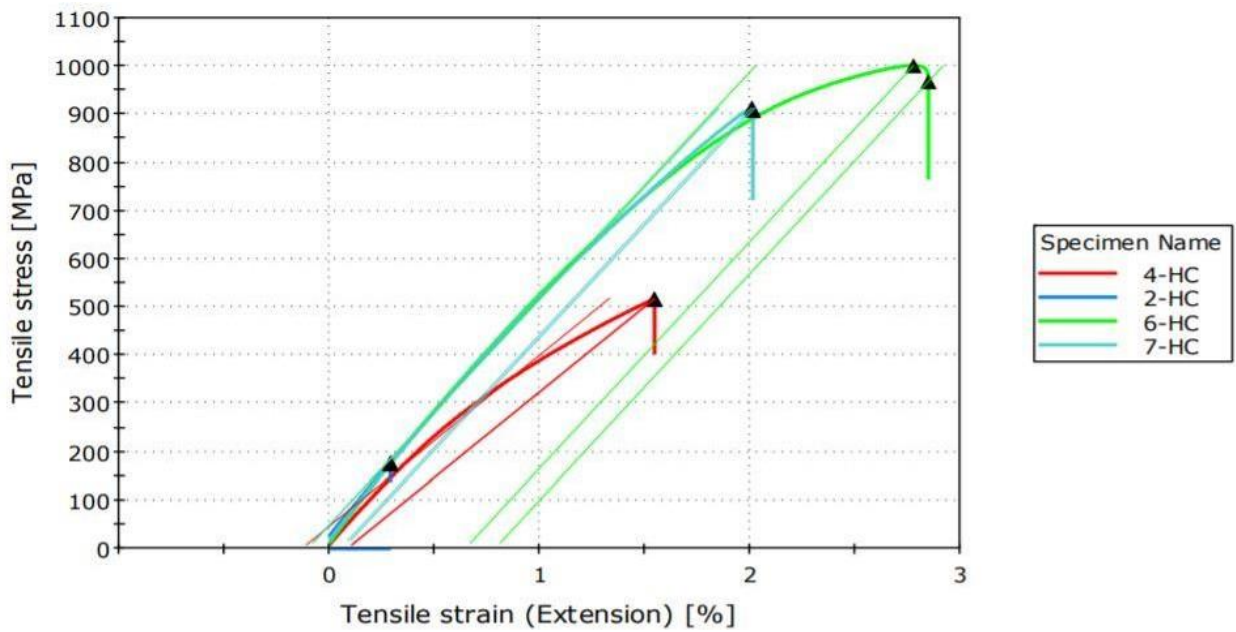


Figure 21 Graph of hydrogen charged sample (Series 3)

Table 11 Tensile strength, and Area reduction of series 3

Serial No.	Temperature	Duration	Tensile Strength	Area Reduction in %
2-HC	Hardened-Tempered350-Charged	314	306	1.9
4-HC	Hardened-Tempered450-Charged	331	568	0.9
6-HC	Hardened-Tempered550-Charged	339	1161	2.8
7-HC	Hardened-Charged	357	1007	0.68

3.3 Comparison of different factors

The reduction in the Cross-sectional area decreases with the decrease in tempering temperature as shown in graph. The hydrogen charges sample were subjected to significant decrement in A%. The ductility (Fracture Strain) of the sample decreases with the increase in the hardness value. Hardness of material increases with the decrease in the tensile strength and tempering temperature increases with the increase in the tensie strength as shown in the figure below.

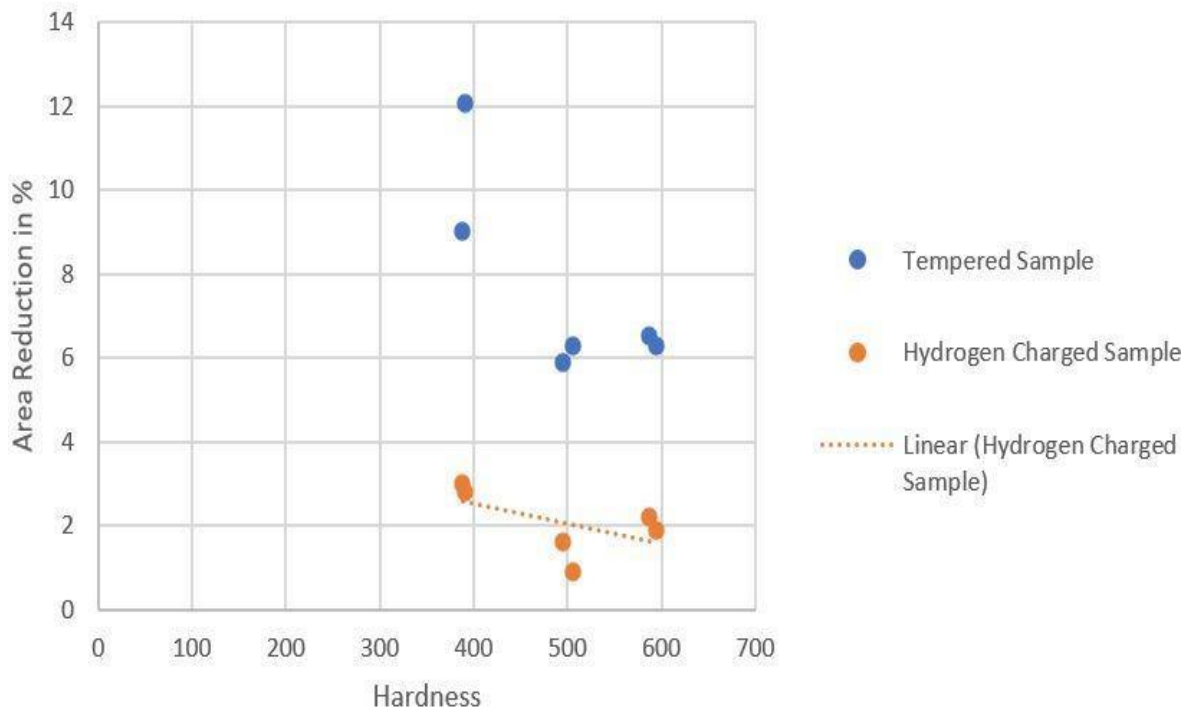


Figure 22 Area Reduction in % vs Hardness

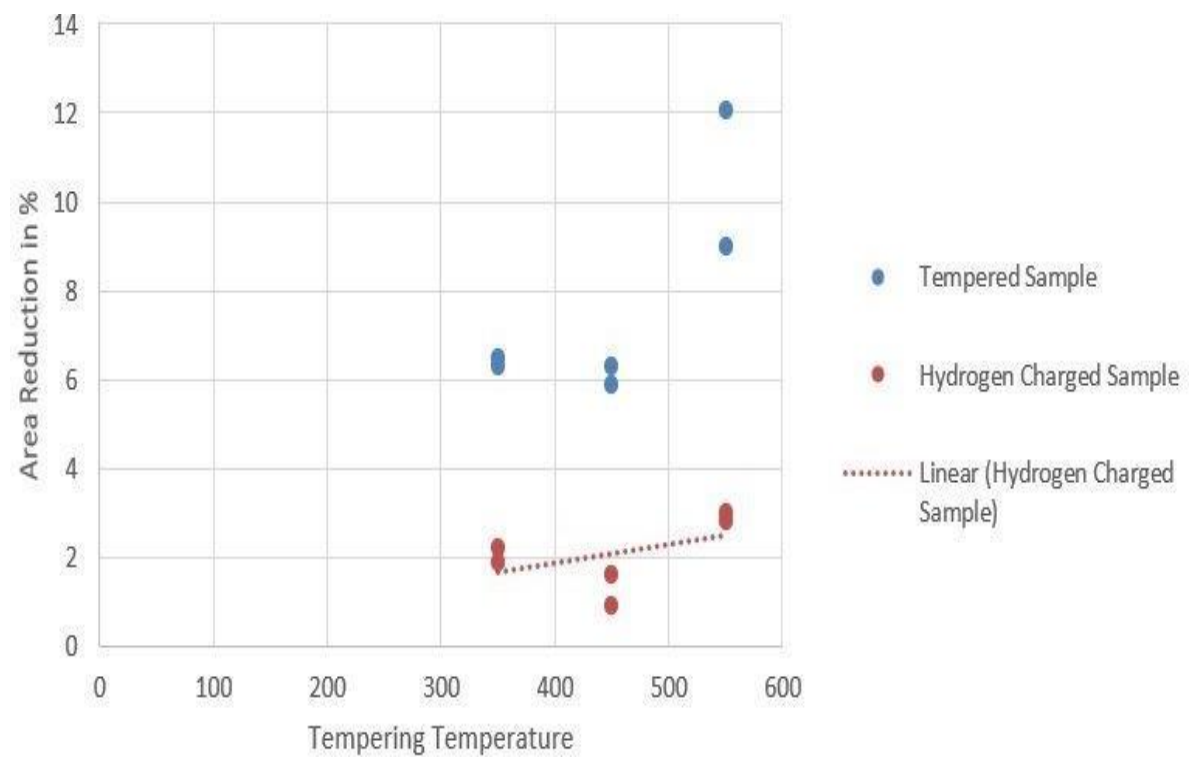


Figure 23 Area Reduction in % vs Tempering Temperature

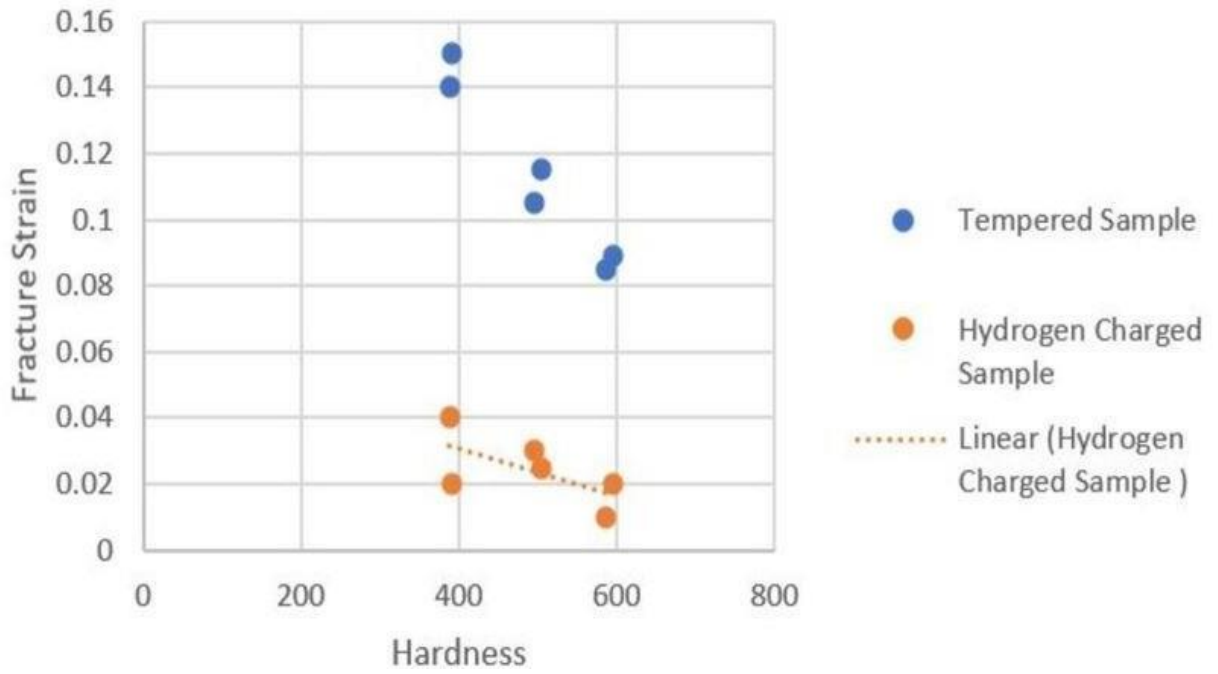


Figure 24 Fracture Strain vs Hardness

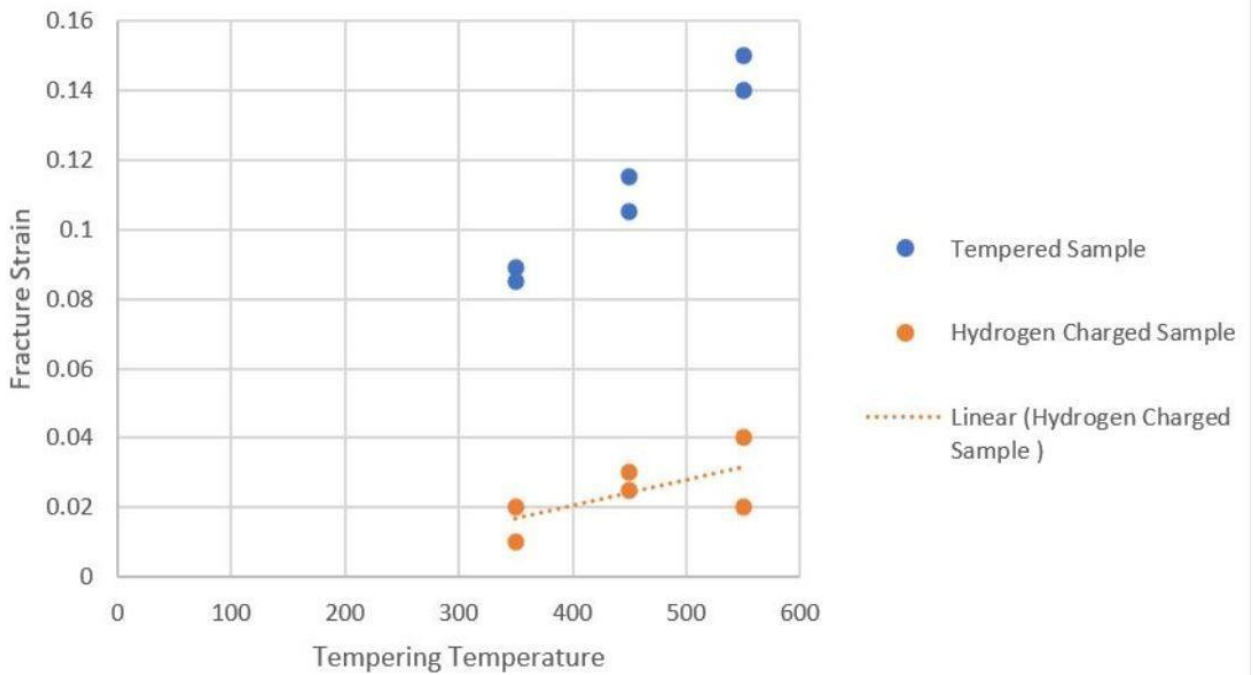


Figure 25 Fracture strain vs Tempering Temperature

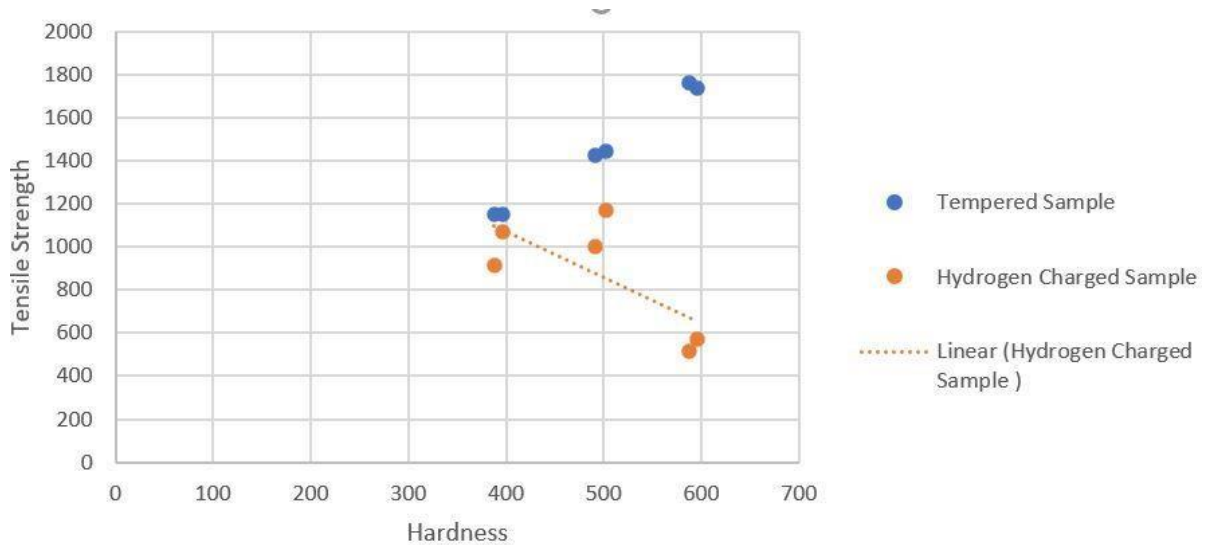


Figure 26 Tensile Strength vs Hardness

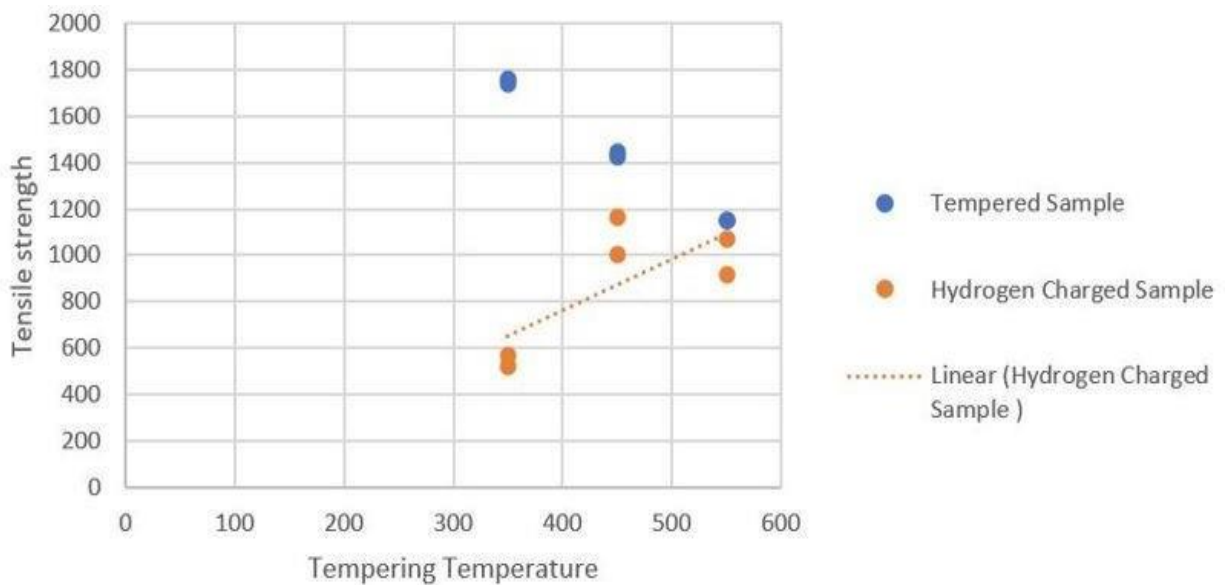


Figure 27 Tensile Strength vs Tempering Temperature

3.4 Susceptibility of hydrogen embrittlement (I_{HE})

The relative HE susceptibility indices (I) are derived for each stress-strain curve of tempered states in relation to the characteristic parameters of the tested samples, Cross-sectional area reduction as a percentage, tensile strength, and fracture. The strain is displayed against the samples' mean HV hardness values well as shown. I_{HE} of the fracture strain and percentage reduction of cross-sectional area ($A\%$) are plotted as a function of hardness and tempering temperature in Figs. 26 and 27, respectively. Mainly Susceptibility index decreases with the increase in hardness. At tempering temperature 450 degree Celsius, there is slight reduce in

susceptibility index as shown in figure 27. But overall there is a uptrend susceptibility index as tempering temperature increases. The formula for calculating susceptibility index in % are as follows

$$I_{HE} \% = (1 - \alpha) \times 100\% \quad \text{where } \alpha = \begin{cases} \frac{\epsilon_{u, ch}}{\epsilon_{u, uc}} \\ \frac{A_{ch}}{A_{uc}} \end{cases}$$

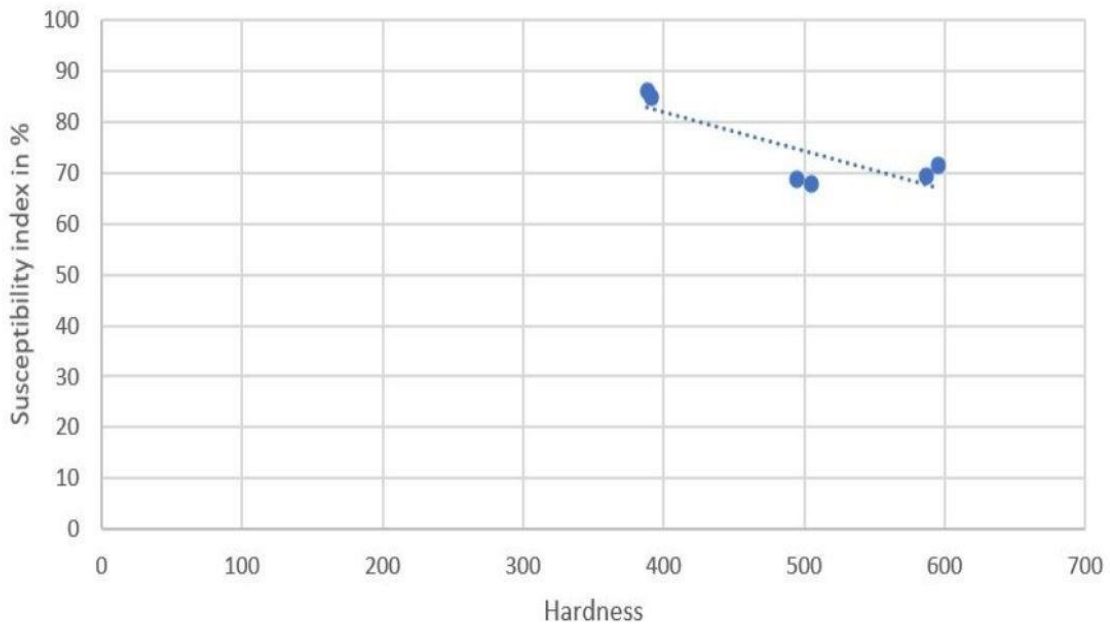


Figure 28 Susceptibility (Area reduction) vs hardness

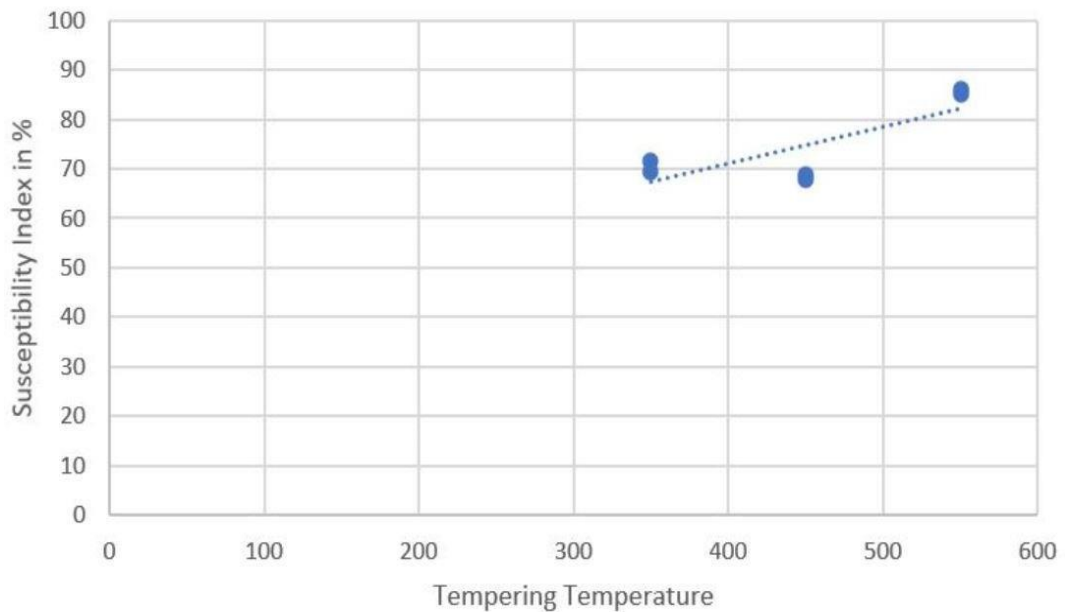


Figure 29 Susceptibility (Area Reduction) vs tempering temperature

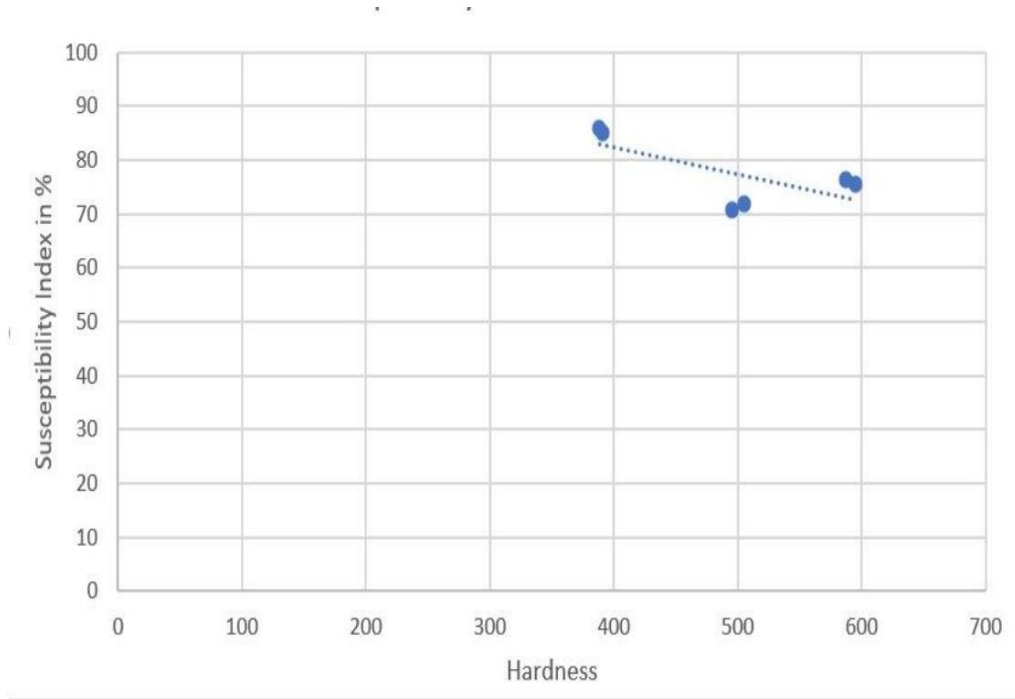


Figure 30 Susceptibility (Fracture Strain) vs hardness

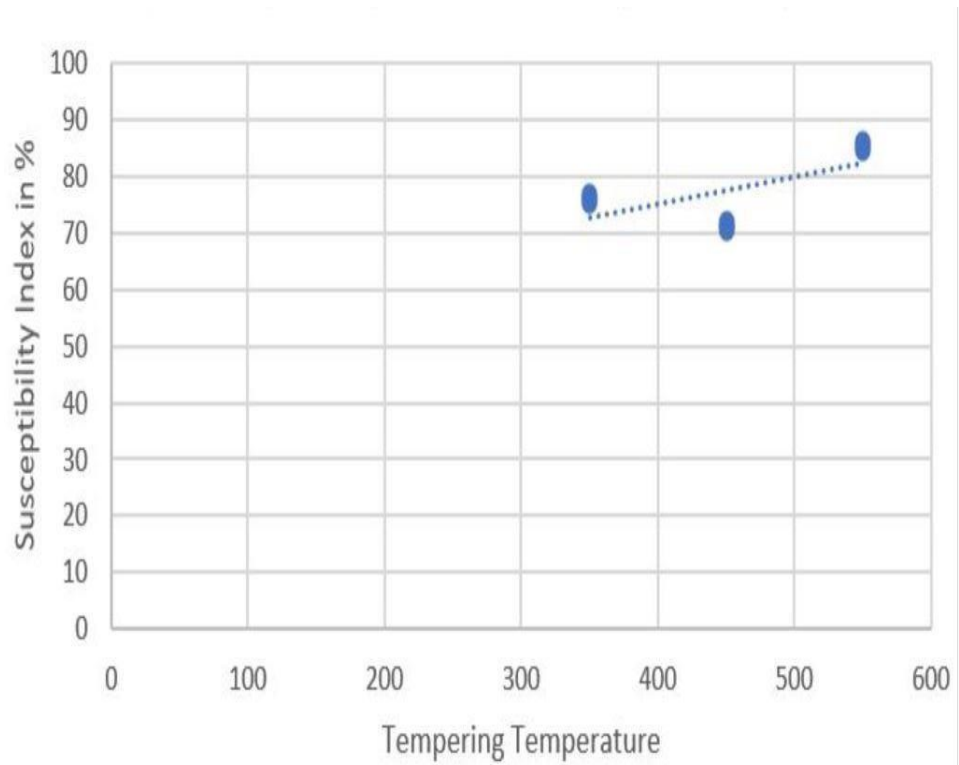


Figure 31 Susceptibility (Fracture Strain) vs Tempering temperature

4. Discussion

A high association between hardness and tempering temperature as well as tempering time has been discovered for the specified alloy (Table 4.1 and Figure 4.3). Furthermore, tensile testing findings (Table 4.2) reveal a substantial link between strength and tempering temperature and the passage of time. The sample that had been quenched (martensitic) had the maximum hardness and strength. Tempering of higher temperature and/or time allowed for a higher amount of carbon precipitation, hence increasing the size of the cementite particles as explained in Section 2.4.2. This resulted in the decrease of strength and hardness as well as increase of toughness as reflected by the results.

4.1 Errors in designing and machining of samples

The design of the tensile rods was considered very carefully at the very onset of the project. Several considerations needed to be evaluated in order to achieve the most fit for purpose design. One feature that early stood out as an important parameter was the length of the tensile rods. The need for sufficient length to accommodate the electrolyte cup with its electrodes, and simultaneously provide enough length to ensure a firm and stable grip in the tensile testing machine.

There was some size differences while cutting samples in band saw machine because it was very hard to make accurate cutting during the process. So there was some differences in the size of samples which is around the tolerance of ± 5 mm. After cutting the raw sample from the piece the next step was to make a shape for a tensile testing in CNC machine. We have used the same program for all specimen. So there might be some variation in the curved size of the specimen which may have created some differences in tensile strength.

4.2 Heat treatment and tempering levels

First, we have prepared some samples and heated at 900°C for 60 minutes. So the hardness value we got was 541 HV then we decided to make more samples and heated at same temperature up to 30 minutes then the hardness value was 675 HV. We proceed with the duration of 30 minutes. The oven was set to 900°C and one specimen was put into the temperature of 550°C and quenched into the oil. The calibration of the oven was checked, using thermocouples. The difference between the displayed temperature and the actual temperature was $\pm 4^{\circ}\text{C}$ at 450°C and $\pm 2^{\circ}\text{C}$ at 550°C during tempering process.

4.3 Hydrogen Charging

The CP and electrolyte setups were done as efficiently and reliably as possible with the resources available for the thesis. However, other than measuring the current and potential, there is no way to know if this experimental procedure succeeded as intended. Since its inception, Tensile testing took between 3 and 13 hours to complete, rather than the expected 24 to 48 hours. The difference in CP incubation time between samples increased after 48 hours. To keep this under control A difference of 17 days was defined as the maximum limit, and a difference of 12 days was set as the lower limit. Then comes the maximum. The difference in incubation time would be approximately 2.5 days. Because of the, this was deemed permissible. This research has a time limit. Talking the results into consideration it would be possible to assume that all samples were charged equally after 12 days, and the difference in hydrogen diffusion above this limit might be negligible. All though there is no current research to back this.

4.4 Slow strain rate test

The SSRT had to be set at a specific speed of . At this rate each test takes several hours, and several factors may influence the result. These factors may include people around the test, unstable electricity to run the machine, software problems and duration of testing. The SSRT is challenging because it is not possible to monitor the entire test due to the duration, especially the SSRT in air. The reason for performing the tensile testing with slow rate is to allow time for the hydrogen to migrate to any crack tip initiating as the specimen is stretched, as elaborated upon in the theory section. This only applies to the samples subjected to HE and tested in electrolyte. For the samples that are tested in air this is not a necessity. There is uncertainty whether the SSRT of 10^{-6} s^{-1} is actually slow enough to allow for proper hydrogen migration to these crack tips.

4.5 Tensile test results

The results from the tensile testing show a clear trend in accordance with the expectations from the theory. The higher temperature the specimens have been tempered at, the more elongation it displays, and also the larger the reduction in area at the point of fracture. Also, the yield strength decreases with higher temperature. In the population of samples there are some that deviate to some extent, but overall the trends observed seem convincing.

5. Conclusion

The main target of this thesis is to find the tensile strength, hardness of AISI 1074 and also find the probability of hydrogen embrittlement. Tensile testing of all three series reveals clear trends. The graphs of tensile stress vs extension and percent RA vs HV hardness show that the electrolyte hydrogen-charged samples were considerably more brittle than the samples evaluated in air. The hardness and strength of the materials varies significantly depending on the time and temperature of tempering. The highest hardness was found in as quenched materials while the lower hardness was found in tempered sample 550 for 60 minutes. Tensile strength of sample 350 was higher among all the samples while the lowest tensile strength was founded in tempered 350.

References

- [1] Dariya Rudomilova, Tomas Prosek, Ines Traxler, Joseph Faderl, Gerald Luckenedar and Andreas Muhr “Critical Assessment of the effect of Atmospheric Corrosion Induced Hydrogen on the Mechanical Properties of Advance High Strength Steel”.
- [2] Xuan Li, “Hydrogen embrittlement II. Hydrogen Effects on X80 Steel Mechanical Properties Measured by Tensile and Impact Testing,” *Physical Review Materials* 1, 033603, 2016.
- [3] R. Gibala and R. F. Hehemann, Hydrogen Embrittlement and Stress Corrosion Cracking, American Society for Metals, 1984.
- [4] N. Eliaz, A. Shachar, B. Tal and D. Eliezer, “Characteristics of hydrogen embrittlement, stress corrosion cracking and tempered martensite embrittlement in high-strength steels,” *Engineering Failure Analysis* 9, pp. 167-184, 2002.
- [5] I. H. Katzarov and A. T. Paxton, “Hydrogen embrittlement II. Analysis of hydrogen-enhanced decohesion across (111) planes in α -Fe,” *Physical Review Materials* 1, 033603, 2017.
- [6] S. Benbelaid, M. A. Belouchrani, Y. Assoul and B. Bezzazi, “Modeling Damage of the Hydrogen Enhanced Localized Plasticity in Stress Corrosion Cracking,” *International Journal of Damage Mechanics*, vol. 20, pp. 831-844, August 2011.
- [7] D. R. Askeland, P. P. Fulay and W. J. Wright, The Science and Engineering of Materials, 6th Edition, 2010.
- [8] J. Song and W. A. Curtin, “Mechanisms of hydrogen-enhanced localized plasticity: Anatomistic study using α -Fe as a model system,” *Acta Materialia* 68, p. 61–69, 2014.
- [9] I. H. Katzarov, D. L. Pashov and A. T. Paxton, “Hydrogen embrittlement I. Analysis of hydrogen-enhanced localized plasticity: Effect of hydrogen on the velocity of screw dislocations in α -Fe,” *Physical Review Materials* 1, 033602, 2017.
- [10] M. Koyama, C. C. Tasan, E. Akiyama, K. Tsuzaki and D. Raabe, “Hydrogen-assisted decohesion and localized plasticity in dual-phase steel,” *Acta Materialia* 70, p. 174–187, 2014.
- [11] M. B. Djukic, G. Bakic, V. Sijacki Zeravcic, A. Sedmak and B. Rajicic, “Hydrogen Embrittlement of Low Carbon Structural Steel,” *Procedia Materials Science* 3, p. 1167–1172, 2014.
- [12] Terje Årthun, Erlend Holm, “Hydrogen Embrittlement of High Strength Carbon Steel,” UiS, 2018.
- [13] Nirosha Adasooriya, Wakshum Tucho, Erlend holm, Vidar Hansen, “Effect of hydrogen on mechanical properties and fracture of martensitic carbon steel under quenched and tempered conditions,” “UiS, 2021.

- [15] D. R. Askeland, P. P. Fulay and W. J. Wright, *The Science and Engineering of Materials*, 6th Edition, 2010.
- [16] W. F. Hosford, "Materials Science an Intermediate Text," Cambridge University Press, 2007, p. 115.
- [17] K. G. Solheim, J. K. Solberg, J. Walmsley, F. Rosenquist and T. H. Bjørnå, "The role of retained austenite in hydrogen embrittlement of supermartensitic stainless steel," *Engineering Failure Analysis* 34, pp. 140 - 149, 2013.
- [18] R. W. K. Honeycombe, "The microstructures of steels," in *Metallography 1963*, The Iron and Steel Institute, 1964, pp. 245 - 305.
- [19] *NS-ISO 6507-1 – Metallic materials – Vickers hardness test.*
- [20] T. S. Aspholm, "Hydrogen Embrittlement of High Strength Carbon Steel," UiS, 2016.
- [21] N. C. Boye, *Kjemi og Miljølære*, Gyldendal undervisning, 2009.
- [22] K. G. Solheim and J. K. Solberg, "Hydrogen induced stress cracking in supermartensitic stainless steels – Stress threshold for coarse grained HAZ," *Engineering Failure Analysis* 32, pp. 348 - 359, 2013.
- [23] U. Kivisäkk, "Influence of hydrogen on corrosion and stress induced cracking of stainless steel - Doctoral Thesis," AB Sandvik Materials Technology R&D, Sweden, 2010.
- [24] R. Francis, *Galvanic Corrosion : a Practical Guide for Engineers*, NACE International, 2001.
- [25] *BS-EN-ISO 7539-7 – Stress corrosion testing.*
- [26] *BS-EN-ISO 7539-11 - Stress corrosion cracking.*
- [27] A. Jemal and M. Birihane, "Hydrogen Embrittlement in High Strength Carbon Steel AISI 4130," UiS, 2017.
- [28] T. S. Aspholm, "Hydrogen Embrittlement of High Strength Carbon Steel," UiS, 2016.
- [29] *NS-EN ISO 6892-1:2009 - Prøvmingsmetode i romtemperatur.*
- [30] Terje Årthun, Erlend Holm, "Hydrogen Embrittlement of High Strength Carbon Steel," UiS, 2018.